

Ferrocene and Half Sandwich Complexes as Catalysts with Iron Participation

René Peters, Daniel F. Fischer, and Sascha Jautze

Abstract The unique and readily tunable electronic and spatial characteristics of ferrocenes have been widely exploited in the field of asymmetric catalysis. The ferrocene moiety is not just an innocent steric element to create a three-dimensional chiral catalyst environment. Instead, the Fe center can influence the catalytic process by electronic interaction with the catalytic site, if the latter is directly connected to the sandwich core. Of increasing importance are also half sandwich complexes in which Fe is acting as a mild Lewis acid. Like ferrocene, half sandwich complexes are often relatively robust and readily accessible. This chapter highlights recent applications of ferrocene and half sandwich complexes in which the Fe center is essential for catalytic applications.

Keywords Catalysis · Ferrocene · Half sandwich complexes · Metallacycles · Planar chirality

R. Peters (✉)

Institut für Organische Chemie, Universität Stuttgart, Pfaffenwaldring 55, D-70569 Stuttgart, Germany

e-mail: rene.peters@oc.uni-stuttgart.de

D.F. Fischer,

Laboratory of Organic Chemistry, ETH Zürich, Wolfgang-Pauli-Str. 10, CH-8093 Zürich, Switzerland

S. Jautze

Institut für Organische Chemie, Universität Stuttgart, Pfaffenwaldring 55, D-70569 Stuttgart, Germany

Laboratory of Organic Chemistry, ETH Zürich, Wolfgang-Pauli-Str. 10, CH-8093 Zürich, Switzerland

Contents

1	Introduction	141
2	Catalysis by Iron in Half Sandwich Complexes	145
2.1	Fe(0)- and Fe(I)-Catalysts	145
2.2	Fe(II)-Catalysts	148
3	Chiral Catalysts Electronically Influenced by a Ferrocene Core	152
3.1	Planar Chiral Ferrocenyl Metallacycle Catalysts	153
3.2	Planar Chiral Ferrocenes as Lewis- or Brønsted-Base Catalysts	163
	References	170

Abbreviations

Å	Ångström
Ac	Acetyl
acac	Acetylacetonate
Ar	Aryl
Bn	Benzyl
Boc	<i>tert</i> -Butyloxycarbonyl
<i>c</i> -	Cyclo-
cat.	Catalytic
CIP	Cahn-Ingold-Prelog
COD	Cyclooctadiene
COP	Cobalt sandwich based oxazoline palladacycle
Cp	Cyclopentadienyl
D	Deuterium
DCE	1,2-Dichloroethane
DCM	Dichloromethane
DME	1,2-Dimethoxyethane
<i>dr</i>	Diastereomeric ratio
<i>ee</i>	Enantiomeric excess
equiv.	Equivalent(s)
Et	Ethyl
h	Hour(s)
Hex	Hexyl
hν	Light irradiation
<i>i</i> -Bu	<i>iso</i> -Butyl
<i>i</i> -Pr	Isopropyl
IUPAC	International Union of Pure and Applied Chemistry
LG	Leaving group
Me	Methyl
Mes	Mesityl, 2,4,6-trimethylphenyl
min	Minute(s)

mol	Mole(s)
mp	Melting point
MTBE	<i>tert</i> -Butylmethylether
Nu	Nucleophile
Pent	Pentyl
Ph	Phenyl
PMP	<i>para</i> -Methoxyphenyl
PS	Proton sponge, 1,8-bis(dimethylamino)naphthalene
R	Residue
rds	Rate determining step
RT	Room temperature
s	Selectivity
SET	Single electron transfer
<i>t</i> -Bu	<i>tert</i> -Butyl
Tf	Trifluoromethylsulfonyl
THF	Tetrahydrofuran
THP	Tetrahydropyranyl
TIPS	Triisopropylsilyl
TMEDA	<i>N,N,N',N'</i> -Tetramethyl-1,2-ethylenediamine
TMS	Trimethylsilyl
Tol	Toluyll
Ts	Toluenesulfonyl
y	Yield
Δ	Reflux conditions

1 Introduction

Ferrocene (**1**) was the first sandwich complex to be discovered, thereby opening a wide and competitive field of organometallic chemistry. The formation of ferrocene was found at almost the same time in two independent studies: on July 11, 1951, Miller, Tebboth, and Tremaine reported that on the passage of N_2 and cyclopentadiene over a freshly prepared mixture of "reduced" Fe (90%), alumina (8%), potassium oxide (1%), and molybdenum oxide (1%) at 300°C, yellow crystals identified as Cp_2Fe (Fig. 1) were obtained [1]. Due to the low yields obtained (3 g starting from 650 g ferric nitrate), doubts remain as to whether Fe(0) was the

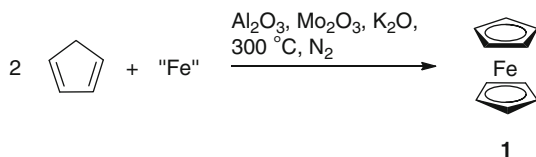
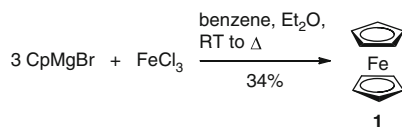


Fig. 1 Formation of Cp_2Fe by Miller, Tebboth, and Tremaine

Fig. 2 Formation of Cp₂Fe by Kealy and Pauson



reactive species or if residual Fe(II) reacted with Cp⁻ formed in situ in the presence of basic oxides.

On August 7, 1951, Kealy and Pauson reported the formation of Cp₂Fe starting from CpMgBr and FeCl₃ (3.5 g from 9.05 g FeCl₃, Fig. 2) [2]. Initially, it was planned to form fulvalene via generation of a cyclopentadienyl radical by SET from Cp⁻ to Fe(III), radical combination and subsequent oxidation of Cp₂ by Fe(III). Instead, Fe(II) formed by reduction with the Grignard reagent reacted further by transmetallation.

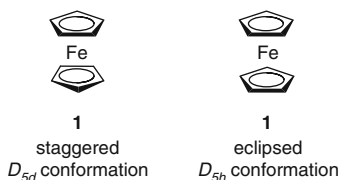
In both original reports, the authors did not assign a sandwich structure to Cp₂Fe. However, their work immediately triggered intensive research activity by other groups to explain the unexpected properties of this new material, culminating in the structure determination as early as 1952 by E.O. Fischer (magnetic studies, X-ray crystal structure analysis) [3, 4], G. Wilkinson, and R.B. Woodward (magnetic studies, IR-spectroscopy) [5].

Due to the aromatic character of Cp₂Fe predicted by Woodward and confirmed by the reactivity toward electrophilic substitutions, which proceed with rates comparable to anisole, the name ferrocene was coined in analogy to simple aromatic systems [6].

A more efficient way to synthesize ferrocene involves a transmetallation of CpNa with FeCl₂ [7]. Ferrocene forms an orange crystalline solid (mp 173°C), which can be purified, for example, by sublimation, and which is relatively inert toward air and hydrolysis [1, 2].

The covalent part of the bonding character of both Cp⁻ ligands with Fe(II) can be summarized by σ -bond interactions (Cp⁻ \rightarrow $s/p_z/d_{z^2}$), strong π -interactions (Cp⁻ \rightarrow $d_{xz}/d_{yz}/p_x/p_y$), and weak retrodonative δ -interactions ($d_{xy}/d_{x^2-y^2} \rightarrow$ Cp⁻) [8]. The molecular orbital interactions are almost independent of the conformation of the sandwich complex with respect to rotation of the Cp rings. Both the staggered (D_{5d}) as well as the eclipsed conformation (D_{5h}) possess similar binding energies [9]. The same holds true for all conformations between these two extremes meaning that the activation energy for ligand rotation is very low (ca. 0.9 ± 0.3 kcal/mol) [10, 11]. In the gas phase the eclipsed conformation is preferred, while for solid state structures of substituted derivatives, preference for one conformation is often due to packing forces or interactions of the various substituents.

All bonding or nonbonding orbitals are filled resulting in a stable diamagnetic 18-electron complex. Single-electron oxidation to a ferrocenium cation provides a 17-electron species, in which one electron is unpaired.



As a consequence of the molecular orbital interactions, ferrocene adopts an axially symmetrical sandwich structure with two parallel Cp ligands with a distance of 3.32 Å (eclipsed conformation) and ten identical Fe–C distances of 2.06 Å as well as ten identical C–C distances of 1.43 Å [12]. Deviation of the parallel Cp arrangement results in a loss of binding energy owing to a less efficient orbital overlap [8]. All ten C–H bonds are slightly tilted toward the Fe center, as judged from neutron-diffraction studies [13].

As mentioned above, ferrocene is amenable to electrophilic substitution reactions and acts like a typical activated electron-rich aromatic system such as anisole, with the limitation that the electrophile must not be a strong oxidizing agent, which would lead to the formation of ferrocenium cations instead. Formation of the σ -complex intermediate **2** usually occurs by *exo*-attack of the electrophile (from the direction remote to the Fe center, Fig. 3) [14], but in certain cases can also proceed by precoordination of the electrophile to the Fe center (*endo* attack) [15].

Due to the pronounced electron donating character of ferrocene, α -ferrocenyl carbocations **3** possess a remarkable stability and can therefore be isolated as salts [16]. They can also be described by a fulvene-type resonance structure **3'** (Fig. 4) in which the Fe center and the α -center are significantly shifted toward each other as revealed by crystal structure analysis, indicating a bonding interaction [17].

Fig. 3 Intermolecular electrophilic substitution reactions of ferrocene via an *exo*-attack

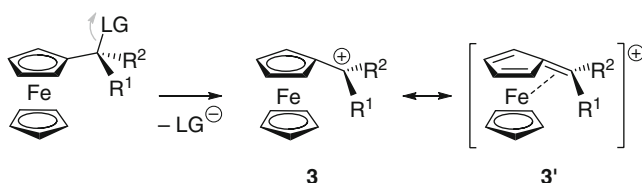
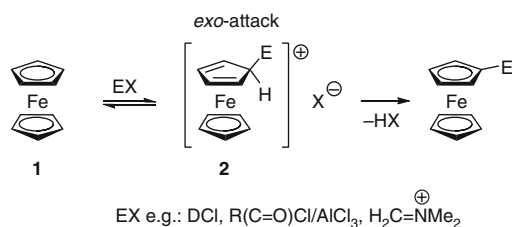
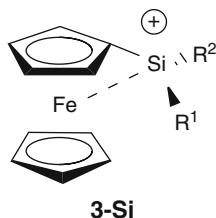


Fig. 4 Formation and stabilization of α -ferrocenyl carbocations **3**

Recently, this concept could be transferred to the homologous silylium ions **3-Si** (Si in α -position to the ferrocene core) [18, 19], which were found to be potent catalysts for Diels–Alder reactions at low temperature [19]. The electron-rich ferrocene core buffers the Lewis acidity, thus avoiding the irreversible formation of Lewis pairs.



Ferrocene derivatives **4** bearing two different substituents $X, Y \neq H$ at the same Cp ring can be planar chiral. Schlögl defined a simple rule to determine the stereodescriptors [20]: looking at the double substituted Cp ring from above, the configuration is defined as R_p if the shortest way through the space starting from the substituent of the highest priority (according to the CIP rules) to the second substituent is clockwise (Fig. 5).

Unfortunately, the IUPAC recommended rule by Cahn, Ingold, and Prelog usually leads to the opposite stereodescriptors [21]. Assuming imaginative Fe–C single bonds between the Fe center and all C atoms, the latter can be treated as distorted tetrahedrons allowing to apply the CIP rules for stereocenters (Fig. 6). The stereodescriptor of the C-atom carrying the substituent of the highest priority is used as stereodescriptor of the whole Cp ring or molecule. As the Schlögl system is more commonly used in literature, it will also be employed in this chapter.

Planar chirality has proven to be a very potent means in asymmetric catalysis to achieve high levels of stereocontrol (see Sect. 3) because planar chiral systems offer

Fig. 5 Definition of the stereodescriptors of planar chiral ferrocenes according to Schlögl

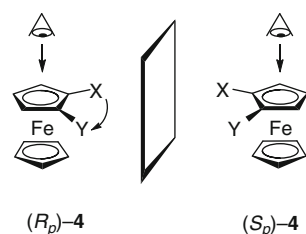
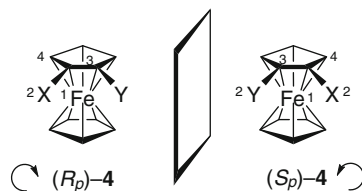


Fig. 6 Definition of the stereodescriptors of planar chiral ferrocenes according to Cahn, Ingold, and Prelog



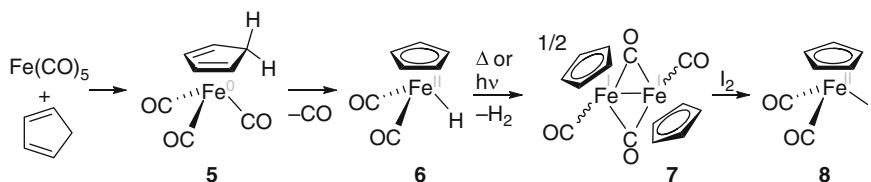


Fig. 7 Formation of the half sandwich complex $\text{CpFe}(\text{CO})_2\text{I}$ (**8**)

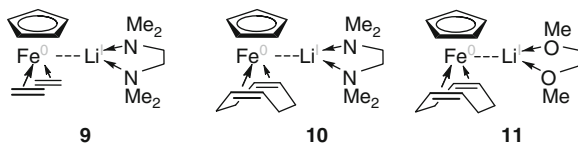
a high degree of spatial control around the active site. The unique and readily tunable electronic and spatial characteristics of ferrocene and ferrocenium systems have been widely exploited in the field of asymmetric catalysis. This is showcased by selected applications in Sect. 3, in which the Fe center communicates with the catalytic site.

Of increasing importance are also Fe half sandwich complexes in which Fe is acting as a mild Lewis acid, presented in Sect. 2. Like ferrocene, half sandwich complexes such as **8** are often relatively robust and readily accessible starting from cyclopentadiene (Fig. 7). Reaction of cyclopentadiene with $\text{Fe}(\text{CO})_5$ initially generates a diene complex **5** which further reacts to give a metal hydride species **6** [22, 23]. The latter can be transformed into dimer **7**, which reacts with oxidizing agents such as iodine to give the synthetically versatile iron prototype half sandwich complex **8** [24]. Section 2 is subdivided into systems with Fe in the oxidation states 0, +I, and +II.

2 Catalysis by Iron in Half Sandwich Complexes

2.1 $\text{Fe}(0)$ - and $\text{Fe}(\text{I})$ -Catalysts

Jonas et al. have shown that individual Cp rings of ferrocene can be successively removed under reducing conditions [25–29]. Working under an ethylene atmosphere, the $\text{Fe}(0)$ half sandwich complex **9** has been formed even on multigram scale as an air-sensitive crystalline solid upon co-complexation of the Li counterion with TMEDA. The labile ethylene ligands can be readily exchanged by the chelating 1,5-cyclooctadiene (COD) forming **10** or the closely related DME adduct **11**.



X-ray crystal structure analysis of **10** and **11** has revealed a close contact between Fe and the Li ion of ca. 2.5 Å. Moreover, the Li ion resides close to the olefin units. Stabilization of the electron-rich Fe center by the π -accepting character of the olefins is evidenced by the significant elongation of the C=C bonds to ca.

1.44 Å in **11** (1.34 Å in free COD). Nevertheless, binding of the olefin ligands is labile enough to allow for ligand exchange, in particular by chelating substrates containing an alkyne moiety, rendering these species attractive as catalysts for cycloisomerizations as demonstrated by Fürstner et al. [30, 31]. In fact, 1,6-enynes **12** undergo an oxidative cyclization pathway, which is triggered by the electron-rich ferrate unit, resulting in a net Alder-ene type cycloisomerization.

While the ethylene ligands in **9** are more readily displaced, COD offers the advantage that it might stabilize the resting state of the catalyst as it stays in solution serving as an ancillary protecting ligand and allowing the cycloisomerization of demanding substrates. It was found that catalyst **9** is particularly suited for the formation of bicyclic products **13** by annulation reactions, in which the size of the preexisting ring of the starting material determines the configuration at the ring junction and displays a distinct influence on the reaction rate (Fig. 8). As a general trend, substrates with larger cycloalkenes usually facilitate the reaction. In the majority of cases, the products were formed as single *trans*-diastereomers with regard to the ring-junction with the exception of [3.3.0]- and [4.3.0]-bicycles **13a** exclusively resulting in a *cis*-arrangement, while decaline products provide *cis/trans*-mixtures. The catalyst has a remarkable compatibility with functional groups and tolerates even terminal alkynes, aryl halides, and tertiary amino groups.

For acyclic enynes, there is a pronounced effect of the substitution pattern on the reactivity (Fig. 9). Substrates **14** with $R^2 = H$ could only be rearranged by catalyst **11**, while **9** failed. For substrates with $R^2 \neq H$, both catalysts were found to be effective providing preferentially the *trans*-configured products **15a**. Enynes carrying trisubstituted olefin moieties failed to react.

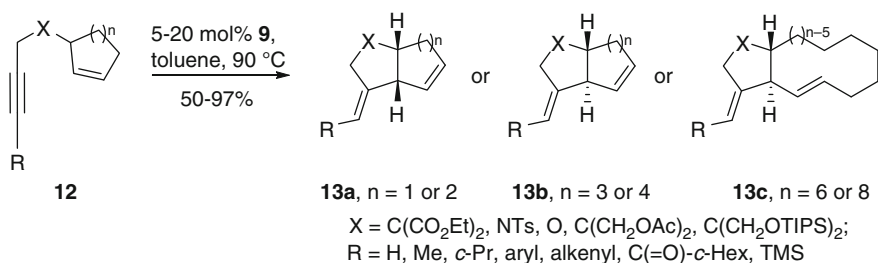
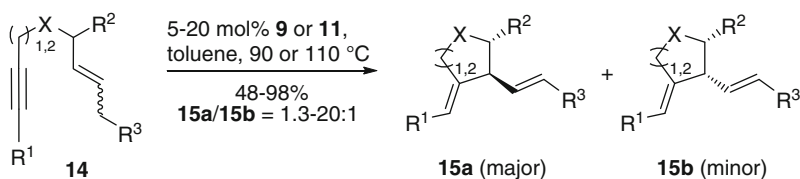


Fig. 8 Cycloisomerizations of cyclic enynes catalyzed by **9**



$X = C(CO_2Et)_2, NTs, NBn, O; R^1 = H, c\text{-Pr, aryl}; R^2 = H, Me, n\text{-Pr, } c\text{-Pr, Ph}; R^3 = H, n\text{-Pr}$

Fig. 9 Cycloisomerizations of acyclic enynes catalyzed by **9** or **11**

Various mechanistic pathways have been considered (Fig. 10), such as addition of a metal hydride species to the alkyne thus forming a vinyl metal complex **16** which subsequently reacts with the olefin part according to a Heck reaction. Alternative scenarios are either an activation of the allylic C-H bond, resulting in a π -allyl species **17**, which subsequently undergoes a metallo-ene like reaction with the alkyne, or an oxidative cyclization of the enyne to generate a metalla-cyclopentene **18**. The product **19** is then released by β -hydride elimination and reductive elimination. To get a more detailed mechanistic insight, D-labeling experiments were conducted, which provide strong evidence for the above-mentioned metalla-cyclic pathway.

Next to cycloisomerizations, catalysts like **11** are also useful for [4 + 2] and even more interesting for [5 + 2] cycloaddition reactions (Fig. 11), which are very

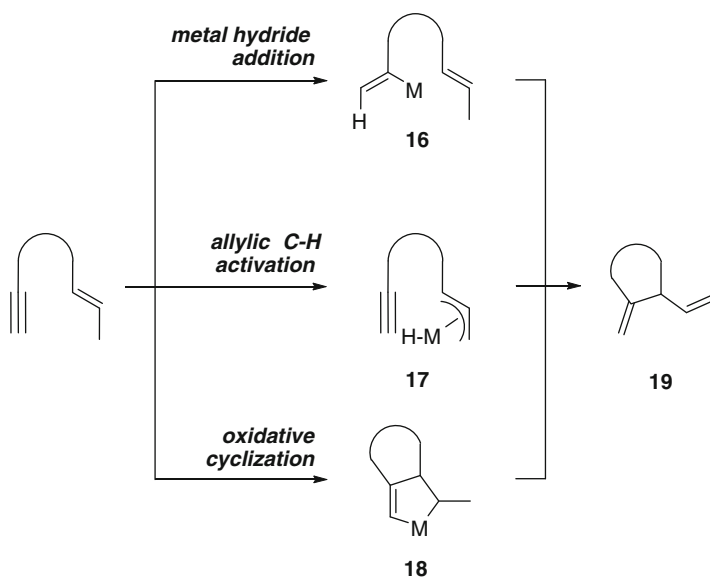


Fig. 10 Mechanistic alternatives for the cycloisomerizations of enynes

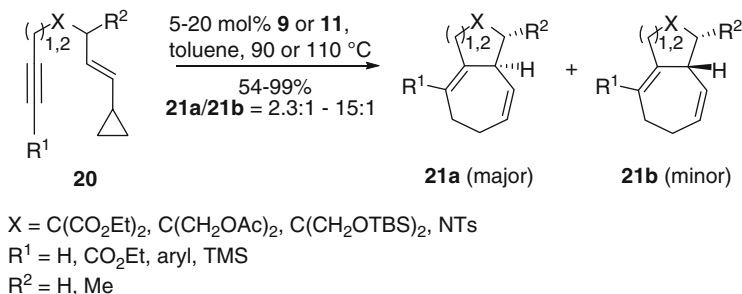


Fig. 11 [5 + 2] cycloaddition reactions catalyzed by **9** or **11**

useful for the formation of seven-membered rings **21** starting from vinyl cyclopropane **20** [31]. Again, **11** was found to be of wider applicability. The cycloheptadiene derivatives were formed with good to excellent diastereoselectivity favoring the 1,2-*trans*-disubstituted diastereomer and tolerating terminal and differently end-capped alkynes. Trisubstituted olefins failed in this approach.

In addition, complexes like **11** are also capable of catalyzing [2 + 2 + 2] cycloadditions of alkyne moieties resulting in the formation of substituted benzenes. Furthermore, Fe(I) catalysts like **22** with an odd electron count (17-electron species) have been studied in this context (Fig. 12) and the initial results demonstrate that they are catalytically relevant, uncovering a previously largely unrecognized aspect.

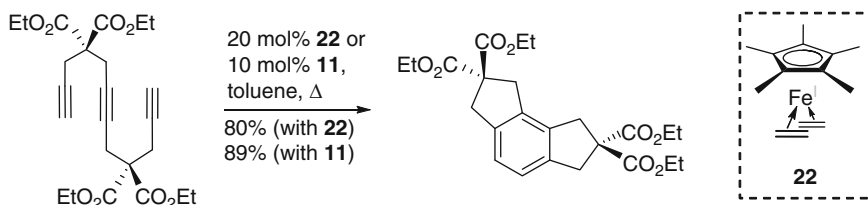


Fig. 12 [2 + 2 + 2] cycloaddition reactions catalyzed by **11** or **22**

A so far unsolved problem is the development of asymmetric procedures for the above described Fe(0)-catalyzed cycloisomerizations and cycloadditions. The option to use the element of planar chirality might allow to successfully address this issue in future applications.

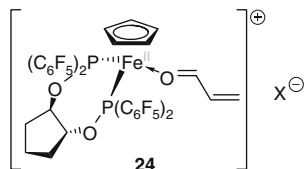
2.2 Fe(II)-Catalysts

Hersh et al. found that the cationic complex $[\text{CpFe}(\text{CO})_2(\text{THF})]\text{BF}_4$ (**23**) can accelerate the [4 + 2] cycloaddition of acrolein and cyclopentadiene [32]. However, the catalytic activity was higher than expected from rate constants determined in stoichiometric experiments, indicating that a Brønsted or Lewis acid impurity might accelerate this process and generating doubts about the role of **23**.

In 1994, Kündig et al. described a related catalyst, in which both CO ligands have been replaced by a chiral *P,P*-chelate ligand providing evidence that structurally defined cationic Fe sandwich complexes are indeed efficient catalysts for Diels–Alder reactions [33].

The Lewis acidity is mainly caused by the positive total charge of complexes like **23** and is further amplified by the π -accepting CO ligands, while the Cp ligand buffers the acidity, overall resulting in mild Lewis acids. Replacement of CO by the less π -acidic PPh_3 resulted in a catalytically inactive species. To retain the catalytic activity, the neutral ligand thus has to mimic the binding characteristics of CO. Accordingly, with $\text{P}(\text{OMe})_3$ catalytic activity was noticed [34, 35]. Kündig et al. utilized a C_2 -symmetric chiral ligand exhibiting similar electronic binding

characteristics as CO as a result of P-bound pentafluorophenyl moieties [36]. Complex **24** can be isolated as a solid by precipitation and can be used as the catalyst precursor, although it was found to be unstable in solution.



24 (5 mol%) catalyzes the cycloaddition of various enals **25**, α,β -substituted or -unsubstituted, and different acyclic and cyclic dienes such as cyclopentadiene with high enantioselectivity favoring in most cases the *exo*-products **26** (Fig. 13). An *endo* product **27** was preferentially formed with cyclohexadiene and a modest *endo* preference was found for the reaction of cyclopentadiene with acrolein. 2,6-Di-*tert*-butylpyridine was usually added to trap Brönsted acid impurities, which otherwise result in reduced *ee* values and varying reaction rates. Reaction temperatures higher than -20°C were not useful as the catalyst slowly decomposes.

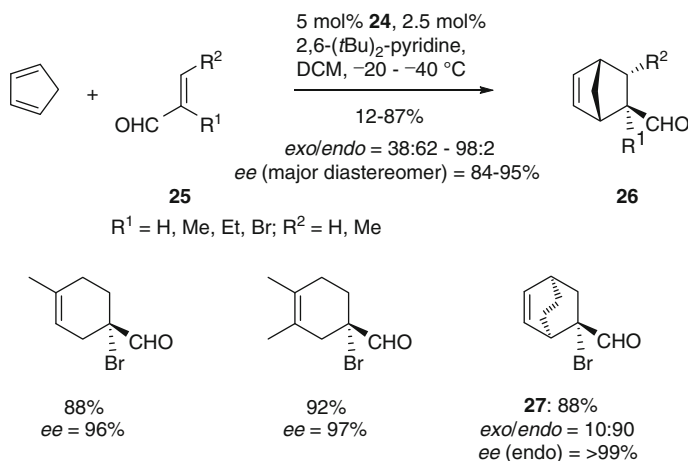
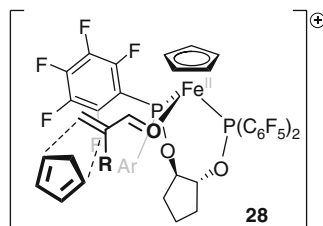


Fig. 13 Diels–Alder reactions with enals catalyzed by **24**

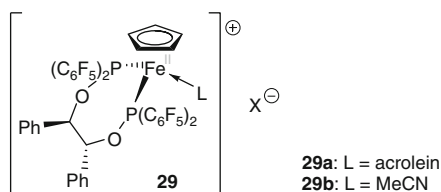
The enantioselectivity was explained by the preference for a transition state **28**, in which the diene approaches the $\text{C}_\alpha\text{-Si}$ face of the coordinated dienophile, which adopts an *s-trans* conformation (Fig. 14).

In 1999, Kündig and Bruin reported a closely related catalyst system **29a**, in which a more readily accessible ligand has been employed [37]. Catalytic activity and stability are strongly dependent upon the nature of the neutral ligand L. While the acetonitrile complex **29b** is stable, yet catalytically inactive, complex **29a** with L = acrolein is stable only in the solid state, but decomposes as a solution in DCM

Fig. 14 Explanation of the enantioselectivity by the preferred transition state **28**



in the absence of an excess of free aldehyde at temperatures above -20°C . Stereoselectivities and yields obtained for the Diels–Alder reaction of enals either match or slightly exceed the results obtained with **24**.



In subsequent work by the same group, a modified procedure for catalyst formation has been developed involving an additional step of anion metathesis thus providing Fe catalysts of higher purity superseding the use of Brønsted acid scavengers.[38] Catalytic activity strongly varies with the counterion, increasing in the order $\text{TfO}^- < \text{BF}_4^- < \text{PF}_6^- < \text{SbF}_6^-$. In general, the Diels–Alder reactions catalyzed by Fe-complexes **24** or **29a** were found to be faster and slightly more enantioselective than with analogous Ru catalysts, which, however, offer the benefit of almost quantitative recovery as directly reusable complexes, while the Fe complexes are too unstable for recovery (for the investigation of the related Ru catalysts, see also [39]).

In addition to asymmetric Diels–Alder reactions, Fe(II) sandwich complexes such as **29a** and their Ru analogues can also be employed as catalysts for asymmetric 1,3-dipolar cycloaddition reactions between nitrones and enals providing isoxazolidines, direct precursors for enantioenriched 1,3-amino alcohols. Usually, Lewis acids coordinate nitrones preferentially (and often irreversibly) over simple α,β -unsaturated aldehydes, explaining the often found necessity of two-point binding dipolarophiles. Any cycloaddition of a mono-coordinating enal with a nitron would thus be due to a noncatalyzed background reaction. Nevertheless, in 2002, Kündig et al. could present the first examples of catalytic asymmetric 1,3-dipolar cycloadditions of nitrones with monocoordinating dipolarophiles based on a judicious choice of the metal ligand environment and Lewis acidity (Fig. 15) [40]. Using **29a** as catalyst (5 mol%), cycloadducts of diarylnitrones were obtained in excellent yield and with high enantiomeric excess. With methacrolein, only *endo*-products were obtained, yet with low regioselectivity. For the acyclic diarylnitrones it was found that the Ru analogous catalysts are superior [41–43].

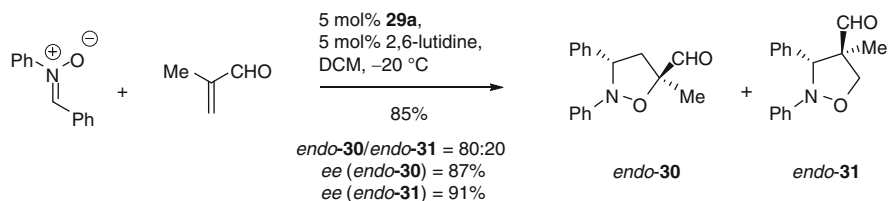


Fig. 15 [3 + 2] cycloaddition reactions of diarylnitrones with enals catalyzed by **29a**

Cyclic N-oxides demonstrated a higher reactivity (Fig. 16). To suppress a thermal background reaction, the nitron concentration had to be maintained low. These conditions afforded the cycloaddition products **32–35** in excellent yields and high enantiomeric purities as a single regioisomer. For cyclic substrates, the Fe-catalyst **29a** performed significantly better than the corresponding Ru analogues. X-Ray crystal structure analysis of the latter as a complex with methacrolein shows that the enal adopts an *s-trans* conformation. The configuration of the cycloaddition products are consistent with an *endo*-approach of the nitron to the C_{α} -*Si*-face of the coordinated enal at the (*R,R*)-catalyst site.

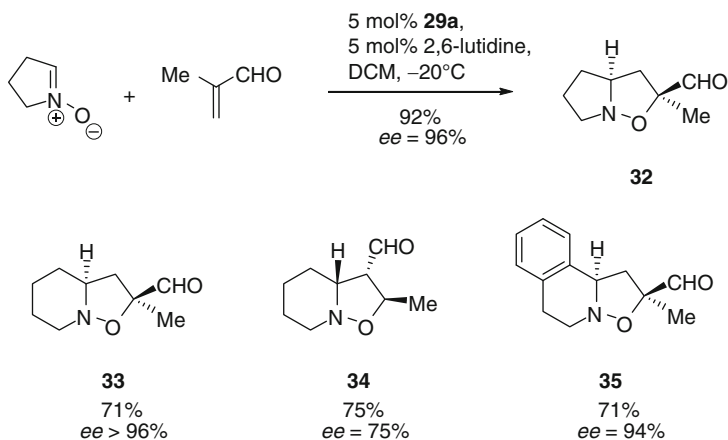


Fig. 16 [3 + 2] cycloaddition reactions of cyclic nitrones with enals catalyzed by **29a**

The cationic complex $[\text{CpFe}(\text{CO})_2(\text{THF})]\text{BF}_4$ (**23**) can also catalyze the proton reduction from trichloroacetic acid by formation of Fe-hydride species and may be considered as a bioinspired model of hydrogenases (“*Fe-H Complexes in Catalysis*”) [44]. This catalyst shows a low overvoltage (350 mV) for H_2 evolution, but it is inactivated by dimerization to $[\text{CpFe}(\text{CO})_2]_2$.

Hydride species were also formed in the dehydrogenative coupling of hydro-silanes with DMF [45]. The catalytic system is applicable to tertiary silanes, which are known to be difficult to be converted into disiloxanes (Fig. 17). The catalytic reaction pathway involves the intermediacy of a hydrido(disilyl)iron complex

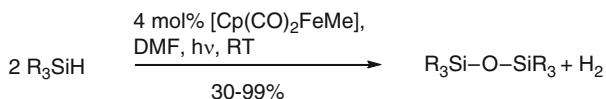


Fig. 17 Dehydrogenative coupling of tertiary silanes

(“*Fe-H Complexes in Catalysis*”). Similarly, also di-*tert*-butyltin dihydride could be dimerized [46].

Cyclopentadienone iron alcohol complexes like **37** were generated from the reactions of [2,5-(SiMe₃)₂-3,4-(CH₂)₄(η⁵-C₄COH)]Fe(CO)₂H (**36**) and aromatic aldehydes [47]. This process can be used for the iron-catalyzed hydrogenation of aldehydes (Fig. 18 and “*Fe-H Complexes in Catalysis*”).

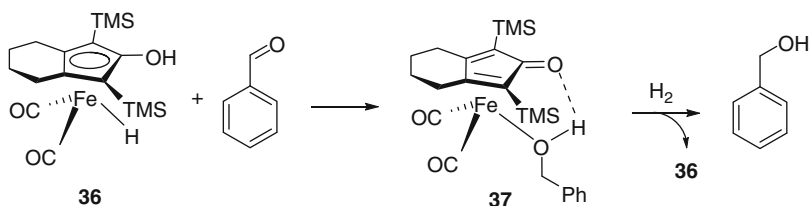


Fig. 18 Iron-Catalyzed Hydrogenation of Aldehydes

The studies described in Sects. 2.1 and 2.2 showcase the high synthetic potential of Fe half sandwich complexes in the field of catalysis and should pave the way for additional exciting developments in the near future.

3 Chiral Catalysts Electronically Influenced by a Ferrocene Core

The ferrocene moiety is not just an innocent steric element to create a three-dimensional chiral catalyst environment. Instead, the Fe center can influence a catalytic asymmetric process by electronic interaction with the catalytic site, if the latter is directly connected to the sandwich core. This interaction is often comparable to the stabilization of α -ferrocenylcarbocations **3** (see Sect. 1) making use of the electron-donating character of the Cp₂Fe moiety, but can also be reversed by the formation of ferrocenium systems thereby increasing the acidity of a directly attached Lewis acid. Alternative applications in asymmetric catalysis, for which the interaction of the Fe center and the catalytic center is less distinct, have recently been summarized in excellent extensive reviews and are outside the scope of this chapter [48, 49]. Moreover, related complexes in which one Cp ring has been replaced with an η⁶-arene ligand, and which have, for example, been utilized as catalysts for nitrate or nitrite reduction in water [50], are not covered in this chapter.

3.1 Planar Chiral Ferrocenyl Metallacycle Catalysts

Palladacycles are defined as compounds with a Pd-C σ -bond with the Pd being stabilized by one or two neutral donor atoms, typically forming 5- or 6-membered rings [51]. Ferrocenyl palladacycles constitute a particularly attractive catalyst class partly due to the element of planar chirality. The first diastereoselective cyclopalladation of a chiral ferrocene derivative was reported in 1979 by Sokolov [52, 53].

There had been doubts about the utility of palladacycles in asymmetric catalysis, raised by the failure to achieve enantioselectivity as a result of a slow release of low ligated Pd(0) (naked Pd) [54]. However, recent success of several planar chiral palladacycles in highly enantioselective *aza*-Claisen reactions and in a number of other applications proves that the coordination shell of the Pd(II) species is not necessarily destroyed during the catalytic action.

3.1.1 The *Aza*-Claisen Rearrangement

In 1997 the first asymmetric *aza*-Claisen rearrangement was reported by Overman et al. [55], which made use of diamines as bidentate ligands for Pd(II), allowing for moderate enantioselectivities. In the same year, Hollis and Overman described the application of the planar chiral ferrocenyl palladacycle **38** as a catalyst for the enantioselective *aza*-Claisen rearrangement of benzimidates **39** (Fig. 19) [56]. A related ferrocenyl imine palladacycle provided slightly inferior results, while a benzylamine palladacycle lacking the element of planar chirality was not able to provide any enantioselectivity [57].

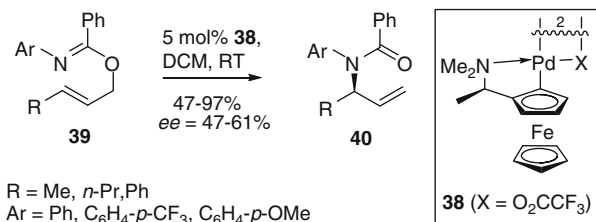


Fig. 19 Asymmetric *Aza*-Claisen Rearrangement of benzimidates **39** using amino palladacycle **38**

A significant breakthrough was achieved by Overman and Donde in 1999: they reported the first highly selective catalyst **41** for the *aza*-Claisen rearrangement of benzimidates **39** (Fig. 20) [58]. Enantioselectivities were in most cases good to very good.

Kang et al. described ferrocene bispalladacycle **42** (Fig. 21) [59]. Enantioselectivities and yields obtained were comparable to the results obtained by Overman with **41** [58].

In 2005, Moyano et al. [60] reported a new type of chiral dimeric ferrocene palladacycle **43** that lacked the element of planar chirality and involved three

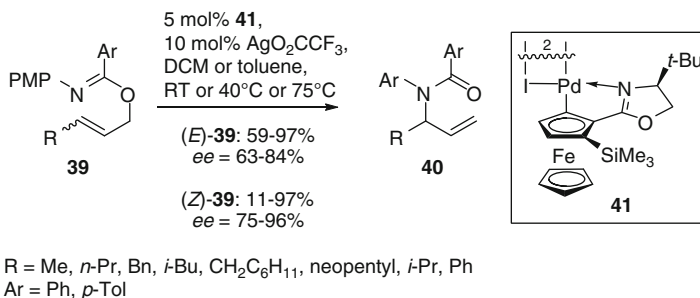


Fig. 20 Asymmetric *aza*-Claisen rearrangement of benzimidates using oxazoline palladacycle precatalyst **41**

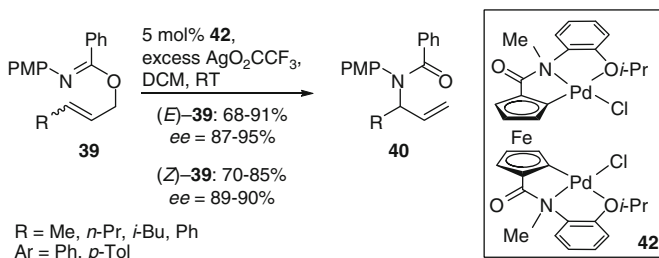


Fig. 21 Asymmetric *aza*-Claisen rearrangement of benzimidates using bispalladacycle precatalyst **42**

Pd-centers as catalysts for the rearrangement of benzimidate substrates. While the enantioselectivity reached a practical value, the yield was only moderate (Fig. 22).

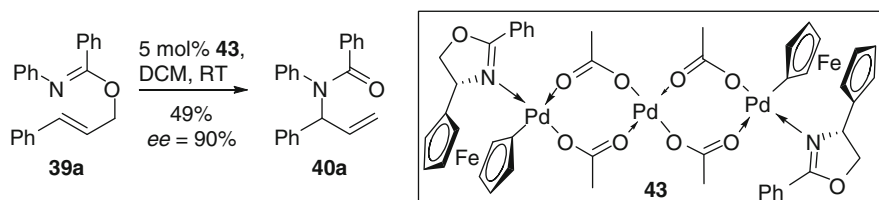


Fig. 22 Asymmetric *aza*-Claisen rearrangement of benzimidate **39a** using the trispalladium species **43**

In 2005 [61], Overman and coworkers described the application of their oxazoline system **41** to synthetically attractive trifluoroacetimidates **44** (Fig. 23) forming trifluoroacetamides **45**, which, in contrast to benzamides **40**, can be readily transferred into free primary allylic amines.

A related planar chiral Co-based oxazoline palladacycle COP-X (**46**) was later found to be of higher synthetic utility as it permitted the use of benzimidates, [62] as well as allylic trifluoro- [63] and trichloroacetimidates [64, 65]. **46** was found to be superior to its ferrocene analogue **41** [61] in a number of aspects such as ease of

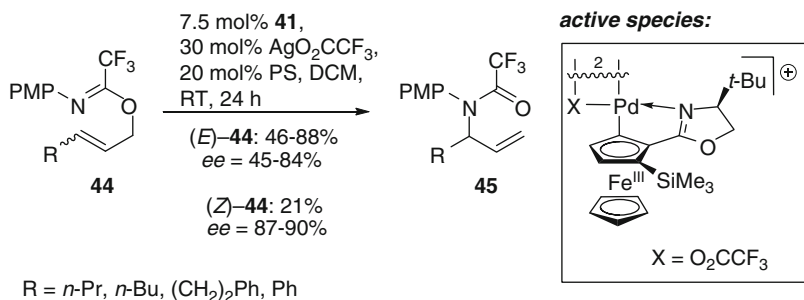
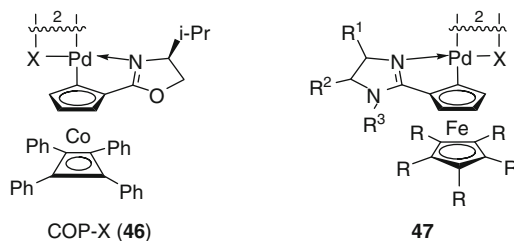


Fig. 23 Asymmetric *aza*-Claisen rearrangement of trifluoroacetimidates using precatalyst **41**

preparation [**41** was not accessible by direct cyclopalladation due to oxidative decomposition by Pd(II)], catalyst stability, activity, and substrate scope.



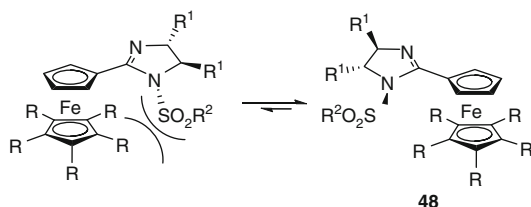
Unfortunately, in the case of trifluoroacetimidates COP-Cl (**46**) still required catalyst loadings, which are not useful for large-scale applications [10 mol% Pd (II)], while long reaction times were necessary for high conversion. Moreover, the scope was limited to substrates bearing α -unbranched alkyl substituents R at the 3-position of the allylic imidate.

Peters and coworkers have systematically addressed the issue of catalytic activity for the asymmetric rearrangement of trihaloacetimidates. These investigations utilized a modular design of a planar chiral carbophilic Lewis acid allowing for an adjustment of electronic and steric properties. Although all previous ferrocene-based catalysts had not been as efficient as COP-X (**46**), ferrocene moieties were chosen as backbone for planar chiral catalyst systems for two main reasons: (a) the cobalt-based sandwich complexes proved to be very sensitive with regard to the cyclopalladation outcome depending on the oxazoline substitution pattern in terms of reactivity and configuration, thus limiting the number of accessible catalyst structures [66]; (b) for the cobalt-based sandwich backbone, the electron density could not be extensively variegated, in contrast to ferrocenes for which, for example, the oxidation potentials are strongly dependent upon the substitution pattern [67].

Along these lines, imidazoline [68, 69] rather than oxazoline coordination sites better fitted into a modular concept in order to understand how the electronic properties should ideally be, since electron density can be readily adjusted by the choice of the N substituent [70]. The Cp' ligand C_5R_5 in **47** permits steric and electronic tuning. With the electron-withdrawing effect of five Ph groups R, the

electron density on the Pd(II)-center is significantly decreased, and the catalyst displays an enhanced Lewis acidity. Additionally, the enhanced bulk has led to an improved enantioselectivity. The iron center of the sandwich moiety can be either Fe(II) or Fe(III). A ferrocenium core formed during catalyst activation via oxidation with a silver salt is in fact a major reason for enhanced catalytic activity as compared to COP (**46**) due to electronic communication with the Pd-center. N-Sulfonyl groups R^3 in **47** resulted in high activity because of their electron-withdrawing effect. The sulfonyl group in **48** offers the additional advantages that Pd can be introduced by a direct diastereoselective cyclopalladation due to enhanced stability of the ferrocene core against oxidative decomposition and owing to a chirality transfer from R^1 to the neighboring N atom effecting a preferred conformation in which the sulfonyl moiety points away from the ferrocene moiety (Fig. 24).

Fig. 24 Conformational equilibrium for **48** caused by chirality transfer to the sulfonylated N-atom



Different counteranions X^- coordinating to the Pd-center of **47a** were employed by breaking the chloro bridge of the catalytically inert dimeric precursor with different silver salts. AgO_2CCF_3 provided the best results. Enantioselectivities were good to excellent and the yields were in general high (Fig. 25). The catalyst loadings could be decreased by a factor of 100 as compared to the previous results, performing catalysis under almost solvent-free conditions.

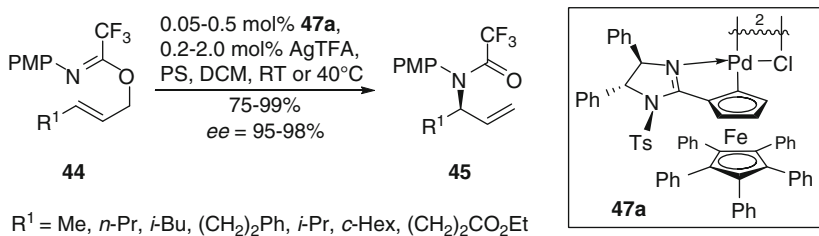


Fig. 25 Asymmetric *aza*-Claisen rearrangement of trifluoroacetimidates **44** using precatalyst **47a**

The high catalytic activity also enabled *aza*-Claisen rearrangements to form *N*-substituted quaternary stereocenters (Fig. 26) [71]. The catalyst does not need to distinguish between differently sized substituents on the double bond of **49** (e.g., $R = \text{CD}_3$, $R^1 = \text{CH}_3$, $ee = 96\%$), indicating that coordination of the olefin is the stereoselectivity predetermining step. The imidate-N-atom subsequently attacks intermediate **47-I** from the face remote to the Pd-center totally resulting in a

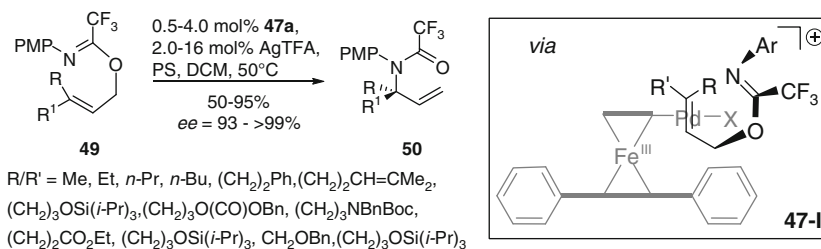


Fig. 26 Asymmetric *aza*-Claisen rearrangement of trifluoroacetimidates **49** generating *N*-substituted quaternary stereocenters

stereospecific reaction outcome. The allylic amides **50** can be transferred to almost enantiopure quaternary α - and β -amino acids. **47a** was also examined for the rearrangement of imidates carrying different *N*-substituents to give rise to various secondary allylic amines after reductive amide cleavage [72].

To examine if the higher catalytic activity and selectivity of **47a** as compared to the COP-X system **46** is mainly caused by the pentaphenyl ferrocenium or by the imidazole moiety, oxazoline **53-Cl** was prepared in diastereomerically pure form starting from carboxylic acid **51** and (*S*)-valinol via oxazoline **52** (Fig. 27) [73].

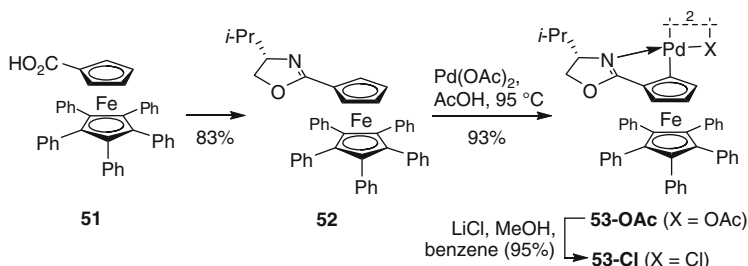


Fig. 27 Synthesis of pentaphenyl ferrocene oxazoline palladacycle precatalyst **53-Cl**

In difference to COP-X (**46**), the *i*-Pr group is pointing toward the sandwich core. AgNO₃ generates a highly active and selective catalyst (Fig. 28). Complete

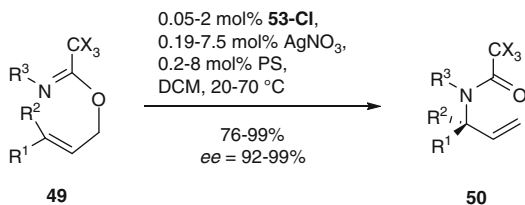


Fig. 28 Asymmetric *Aza*-Claisen rearrangement using precatalyst **53-Cl**

$R^1 = n\text{-Pr, Me, } (\text{CH}_2)_2\text{Ph, } (\text{CH}_2)_3\text{OTIPS, } i\text{-Pr, } c\text{-Hex, Ph,}$
 $p\text{-ClC}_6\text{H}_4, p\text{-MeC}_6\text{H}_4, p\text{-CF}_3\text{C}_6\text{H}_4$
 $R^2 = \text{H, Me, CH}_2\text{OBn; } R^3 = \text{PMP, Ph, } c\text{-Hex, H; X = F, Cl, H}$

oxidation to the corresponding catalytically active ferrocenium species is accomplished with 4 equiv. of AgNO_3 per Cl-bridged dimer. **53-Cl** activated by AgNO_3 is in general more reactive than **47a** still allowing for almost perfect stereocontrol.

The steric environment of COP-X **46** and **47a** around the catalytic palladium site mainly differs in a Ph (**47a**) and an *i*-Pr group (**46**) next to the coordinating N-site and the type and distance of the spectator ligand. While the distance of the two sandwich ligands differs only slightly between COP and **47a** (3.4 Å vs. 3.3 Å), oxidation of the ferrocene to a ferrocenium species is expected to shorten this distance further. Overall, the steric hindrance to access the Pd-center is more distinct for **47a**. These steric effects are capable to explain the higher *ee* obtained with **47a**.

From an electronic point of view, the differences are more pronounced since the overall charge of the ligand (−1 for COP, 0 for **47a** after oxidation to the ferrocenium species) changes. As Pd(II) most likely acts as a carbophilic Lewis acid coordinating to an olefin, the lower electron density in **47a** is suitable to explain the higher reactivity found for this complex.

When comparing COP-X **46** to oxazoline **53-Cl**, there are two major differences: (1) the *i*-Pr residue on the oxazoline moiety in **53-Cl** is pointing toward the Cp'-spectator ligand, leaving the space above the Pd square plane unhindered, while in COP, the substituent is pointing away from the sandwich core. (2) **53-Cl** can be oxidized to a ferrocenium species, again providing a less electron-rich ligand.

The origin of the higher rate of **53-Cl** as compared to **47a** might be explained by the better accessibility of the Pd^{II}-center in the former, as the *exo*-face above the Pd-square plane is open thus resulting in a facilitated olefin coordination via an associative mechanism. Since the *ee*-values obtained with **53-Cl** are practically identical to those obtained with **47a**, enantioselectivity originates nearly exclusively from the planar chiral pentaphenyl ferrocene backbone.

Geometrically pure substrates are needed to obtain high enantioselectivities due to the stereospecific reaction outcome. **53**, however, is less active for *Z*-configured allylic imidates. As *Z*-olefins are, in general, more readily available in isomerically pure form, for example by semihydrogenation of triple bonds, this substrate class would be more interesting for technical applications. To develop a catalyst highly active for *Z*-configured substrates, the electron density of the second Cp ligand was further decreased, yet avoiding a complicated catalyst preparation for practical reasons. Ferrocene bisimidazoline bispalladacycle **55** fulfills these requirements. The ligand preparation requires only three steps from ferrocene taking advantage of the C_2 symmetry (Fig. 29). Ligand **54** undergoes a diastereoselective biscyclopalladation [74–76].

55 is to date the only highly active enantioselective catalyst for the *aza*-Claisen rearrangement of (*Z*)-configured trifluoroacetimidates (*Z*)-**44** (Fig. 30) [74, 75]. The rearrangements, which proceed, in general, under almost solvent-free conditions, were found to be equally effective on mg- and g-scale and tolerant to many important functional groups. The monomeric structure of the active catalyst species **56**, which is in this case not a ferrocenium species, was determined by NMR.

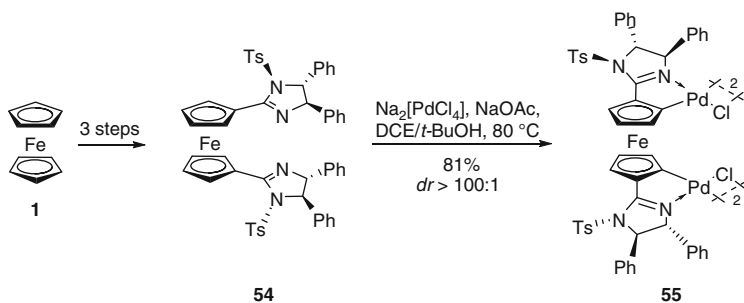


Fig. 29 Formation of **55** via direct diastereoselective biscyclopalladation

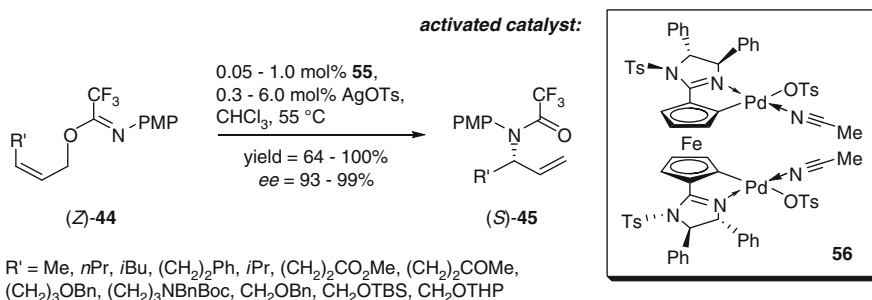


Fig. 30 Asymmetric *aza*-Claisen rearrangement of (*Z*)-configured trifluoroacetimidates **44**

3.1.2 Bispalladium-Catalyzed Michael-Addition of α -Cyanoacetates

Ferrocene-1,1'-diylbismetallacycles are conceptually attractive for the development of bimetal-catalyzed processes for one particular reason: the distance between the reactive centers in a coordinated electrophile and a coordinated nucleophile is self-adjustable for specific tasks, because the activation energy for Cp ligand rotation is very low. In 2008, Peters and Jautze reported the application of the bis-palladacycle complex **56a** to the enantioselective conjugate addition of α -cyanoacetates to enones (Fig. 31) [74–76] based on the idea that a soft bimetallic complex capable of simultaneously activating both Michael donor and acceptor would not only lead to superior catalytic activity, but also to an enhanced level of stereocontrol due to a highly organized transition state [77]. An α -cyanoacetate should be activated by enolization promoted by coordination of the nitrile moiety to one Pd(II)-center, while the enone should be activated as an electrophile by coordination of the olefinic double bond to the carbophilic Lewis acid [78].

The loading of the activated monomeric catalyst could be decreased to a level of 0.04 mol% for certain substrates [turn over number: 2,450]. The developed process does not require the use of inert gas techniques and in most cases chromatographic purification was not necessary to obtain analytically pure products as no side products were formed and the catalyst could be separated by filtration.

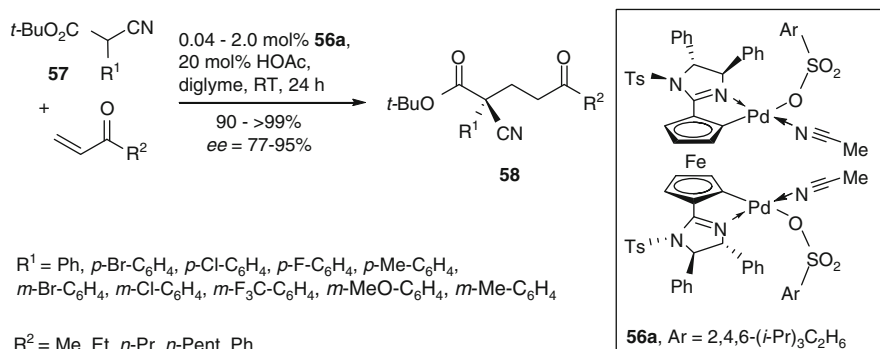


Fig. 31 Bis-Pd(II)-catalyzed asymmetric Michael addition of α -cyanoesters **57** to enones

Kinetic, spectroscopic, and enantioselectivity data provided strong evidence for a mechanism involving bimetallic catalysis. The configurational outcome depends upon the face selectivity of the enol approaching the Michael acceptor in **59** (Fig. 32). To differentiate between the enantiotopic faces, the catalyst has thus

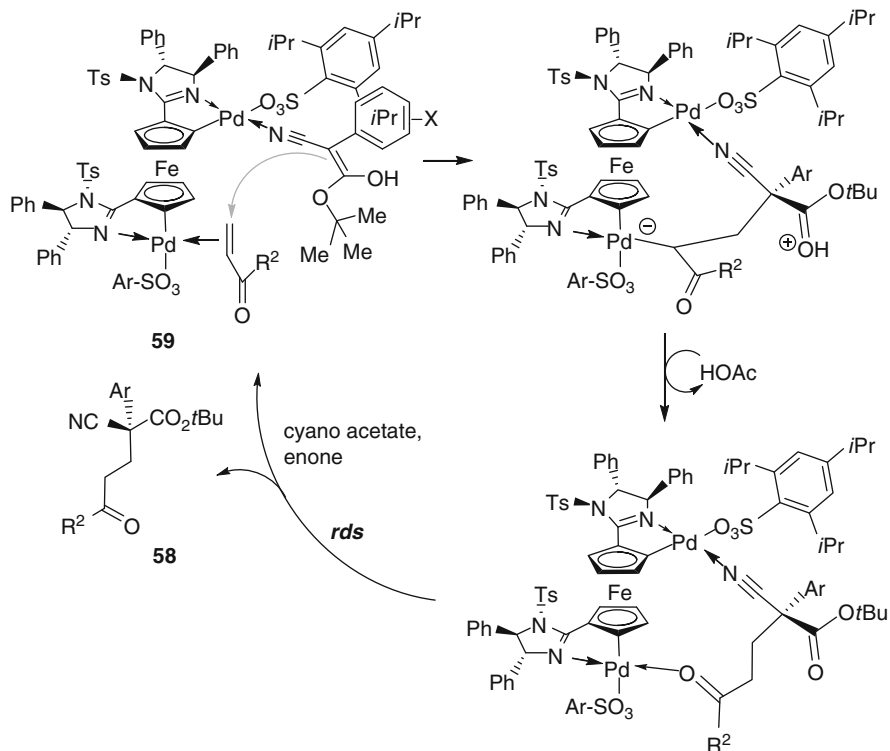


Fig. 32 Proposed cooperative bimetallic intramolecular mechanism for the enantioselective Michael addition of α -cyanoesters **57** to vinylketones

(a) to control the conformation of **59** with regard to the C–CN σ -bond and (b) to direct the enone. Control of the reactive conformation is achieved by the use of a bulky ester moiety and an especially large sulfonate counteranion. The direction of the enone attack is accomplished by the cooperative mechanism as control experiments have shown. Using the corresponding mono-palladacycle, the product was formed with low and inversed enantioface selection due to preferential attack of MVK on the *Re*-face of the enol.

The initial rate of the model reaction follows a first-order dependence for the activated catalyst, the Michael donor, and the Michael acceptor. The rate determining step is not the C–C bond formation or protonolysis but the decomplexation of the bidentate product. This was evidenced by the relationship between the initial conversion and the reaction time. Extrapolation to $t_0 = 0$ h provides a positive intercept. In other words, upon addition of the reagents, the C–C bond formation occurs almost instantaneously. The amount of product at t_0 correlates within the experimental error to the double precatalyst loading since the dimeric precatalyst forms two active monomeric catalyst species.

3.1.3 Ferrocene Bisimidazoline Platinacycle-Catalyzed Intramolecular Friedel–Crafts Alkylations

Ligand exchange processes are relatively slow with Pt [79, 80]. Pt-catalysts allowing for a more rapid ligand exchange could therefore lead to enhanced activity. A mono-platinacycle complex **60** was thus designed in which the Pt-center binds to two imidazoline units: one connected to the same Cp plane as the metal, the second one to the Cp' ligand resulting in severe structural distortion [81]. Cycloplatination of bisimidazoline **54** (Fig. 33) occurs on treatment with $K[(H_2C=CH_2)PtCl_3]$. Both imidazoline units bind in a *trans*-mode to the same Pt entity resulting in a unique geometry in which the C-atom connected to the metal center is strongly pyramidalized (angle Cp–Pt: 159° , deviation of Pt from the upper Cp plane: 0.74 Å). The Cp rings are strongly tilted toward each other resulting in a close contact between Pt and Fe (3.19 Å). The conformational freedom of ligand **54** with regard to rotation

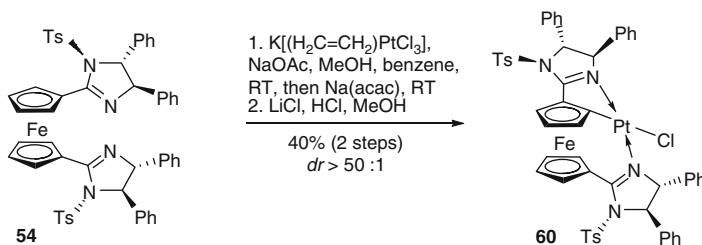


Fig. 33 Formation of platinacycle **60** by direct diastereoselective cycloplatination

along the Fe–Cp axes in combination with the possible deviation from the nonparallel Cp orientation are crucial factors to allow for such catalyst geometry.

To establish proof of principle, the intramolecular Friedel–Crafts alkylation with unactivated olefins was selected (Fig. 34). Platinacycle **60** is in fact sufficiently active to catalyze this process for the first time with indole systems **61** carrying a disubstituted olefin moiety. The highest reactivity was attained by activating **60** with $\text{AgO}_2\text{CC}_3\text{F}_7$ delivering the targeted products **62** in good yield and with high *ee* values. The corresponding nondistorted platinacycle with only one imidazoline unit provided product in poor yield under identical reaction conditions.

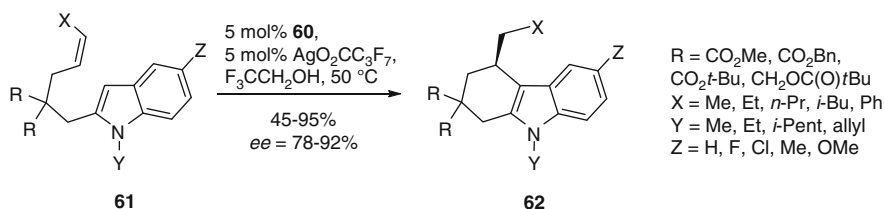


Fig. 34 Catalytic asymmetric Friedel–Crafts alkylation of indoles catalyzed by **60**

Both electron-withdrawing and -donating substituents Z on the aromatic nucleus afforded smooth conversion and similar enantioselectivity despite the projected difference in indole nucleophilicity.

The high enantioselectivity again can be rationalized by enantioface-selective alkene coordination in **63** (Fig. 35). The olefin moiety is expected to bind *trans* to the upper imidazoline moiety [70, 73] thereby releasing the catalyst strain. Coordination at this position may, in principal, afford four different isomers assuming the stereoelectronically preferred perpendicular orientation of the alkene and the Pt(II) square plane. In the coordination mode shown, steric repulsion between both olefin substituents and the ferrocene moiety is minimized. Outer-sphere attack of the indole core results in the formation of the product's stereocenter.

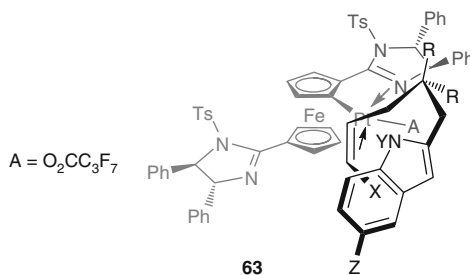
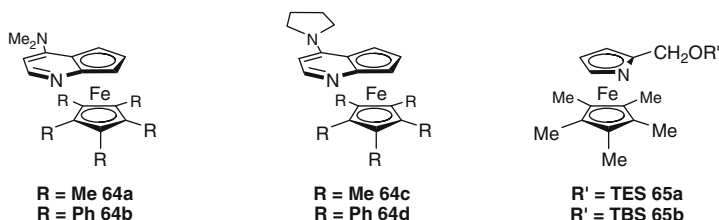


Fig. 35 Explanation of the enantioselectivity by face selective olefin coordination

3.2 Planar Chiral Ferrocenes as Lewis- or Brønsted-Base Catalysts

In 1996, Fu et al. reported the synthesis of the planar chiral heterocycles **64**, formally DMAP fused with a ferrocene core [82]. While the original synthesis provided racemic **64a** in only 2% overall yield requiring a subsequent resolution by preparative HPLC on a chiral stationary phase, a recently improved synthesis furnished the racemic complexes **64** in 32–40% yield over seven steps. A subsequent resolution with di-*p*-toluoyltartaric or dibenzoyltartaric acid gave access to the enantiomers with >99% *ee* (28–44% yield for each isomer in this step) [83].



The [Fe-Cp]-fragment does not only play the role of an additional steric element introducing planar chirality into the otherwise flat pyridine system. Substitution at the pyridine 2-position usually cuts the nucleophilicity of the nitrogen atom thus limiting the possibilities to achieve efficient chirality transfer using nucleophilic pyridine catalysts [84]. Ferrocene, however, functions as a strong electron donor (see Sect. 1) and thus restores the nucleophilicity impaired by substitution.

Extending the same concept of a planar chiral nucleophilic or basic heterocyclic Fe-sandwich complex, *aza*-ferrocenes **65** were prepared. The latter have also been successfully applied as bidentate ligands in transition metal catalysis [85].

Complexes like **64** and **65** can act by two general ways: either as a Brønsted-base or as a nucleophilic catalyst, depending on the type of reaction and substrate. However, the exact mechanistic pathway is in a few cases speculative to some extent as the distinction between the two mechanistic routes is sometimes rather difficult.

3.2.1 Brønsted-Base Catalysis

64a/c is, mainly due to the electron-donating nature of the pentamethyl ferrocene core, a comparatively strong base capable of deprotonating acidic compounds RX-H like phenols [86], hydrazoic acid [87], or 2-cyanopyrrole [88]. The generated corresponding anionic base RX^- can then undergo addition to a disubstituted ketene **66** (Fig. 36) to form a prochiral enolate **67** which is subsequently protonated by **64-H**⁺ in an enantioselective manner.

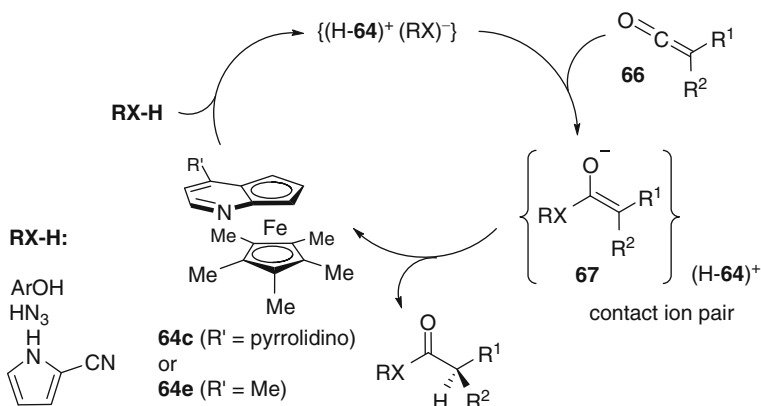


Fig. 36 Catalytic cycle for the Brønsted-base catalyzed addition of phenols, hydrazoic acid, or 2-cyanopyrrol to ketenes

To ensure that proton transfer takes place from the protonated catalyst **64-H⁺** and not from the acidic reagent itself, apolar solvents favoring contact rather than solvent separated ion pairs as well as a slow addition of the acidic substrate RX-H are required. In addition, it was sometimes found beneficial to lower the basicity of the catalyst, thus rendering the protonated species [catalyst-H⁺] more acidic for the stereo-determining protonation of the enolate. This was accomplished by formally replacing NR_2 by Me (see **64e**, Fig. 36).

Employing this method, enantioenriched phenol esters **68**, amides **69**, and carbamates **70** (after Curtius rearrangement of the intermediate acyl azide) were prepared in yields often greater than 90% with *ee*-values reaching up to 97% (generally 80–95%, see Fig. 37).

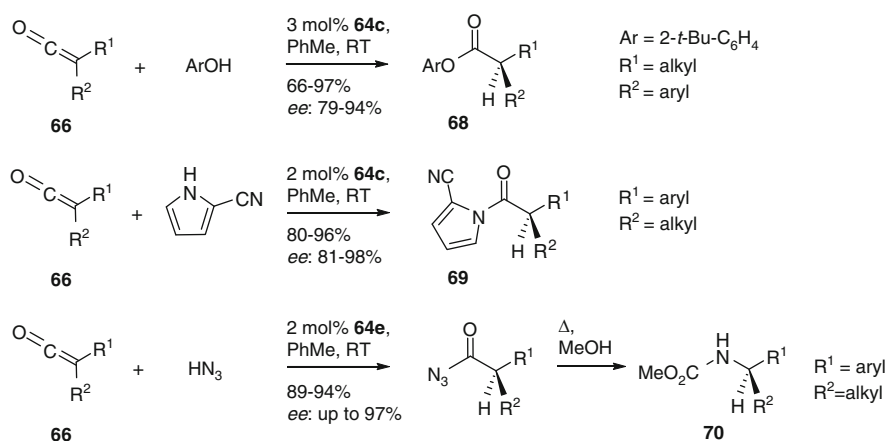


Fig. 37 Addition of phenols, 2-cyano-pyrrol, or hydrazoic acid to ketenes

3.2.2 Lewis-Base Catalysis via Intermediate Formation of a Chiral Zwitterionic Enolate

In an alternative mode of catalyst action, a disubstituted ketene **66** initially suffers a nucleophilic attack of **64**, leading to zwitterionic enolate **71** (Fig. 38).

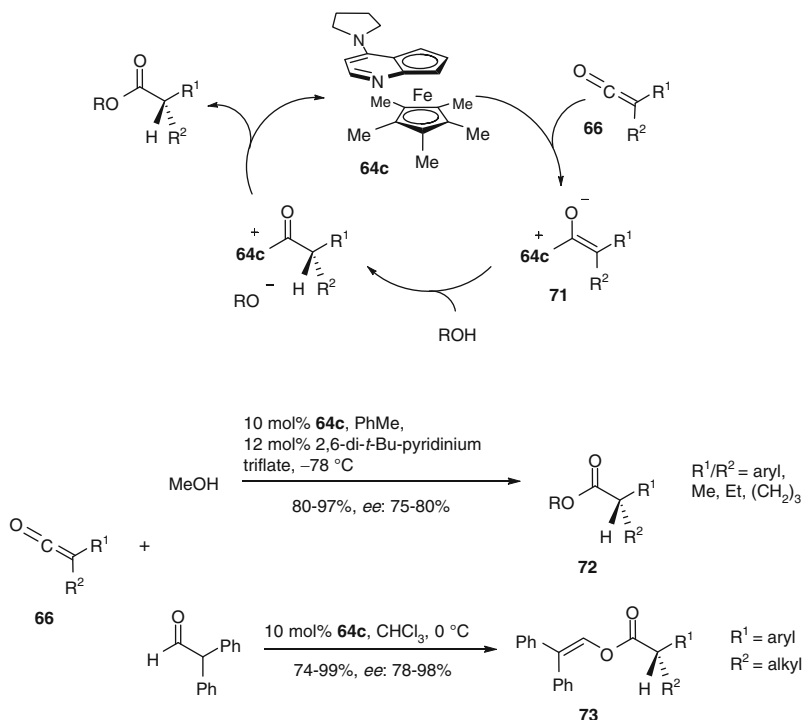


Fig. 38 Formation of chiral esters via zwitterionic enolates

This enolate can then react with a plethora of electrophiles, setting a new stereocenter by a diastereoface-selective reaction. The simplest electrophile to trap enolate **71** is H^+ , which can, for example, originate from methanol [89] or diphenyl acetaldehyde (as a readily enolizable aldehyde) [90] leading to the acylated catalyst species (Fig. 38). The free catalyst is regenerated by acyl-group transfer to methanol(ate) or the aldehyde-derived enolate, producing methyl or enolesters **72/73** in good yields and enantioselectivities.

In a related reaction, enolate **71** is undergoing an electrophilic chlorination with 2,2,6,6-tetrachloro-cyclohexanone (**74**, Fig. 39), eventually leading to α -chlorinated enol esters **75** [91]. However, a different mechanism cannot be completely ruled out, where the catalyst is not acylated by the ketene, but chlorinated by the tetrachloro-ketone to form $[\mathbf{64c}\text{-Cl}]^+$ as the reactive species.

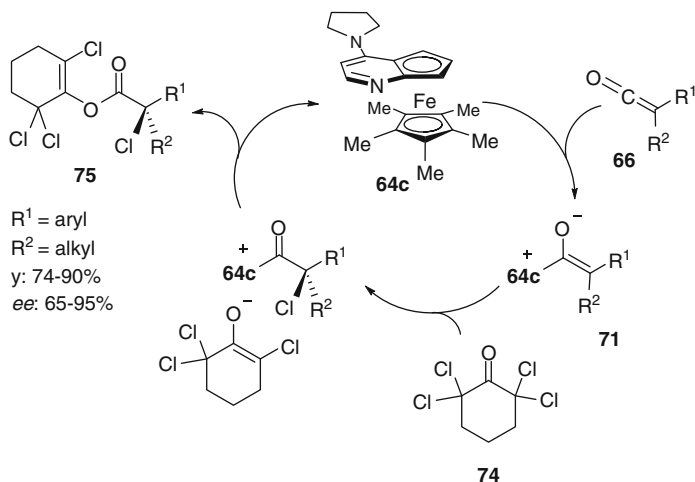


Fig. 39 Chlorination

3.2.3 Formal [2 + 2]-Cycloadditions

The Staudinger reaction [92], a [2 + 2]-cycloaddition of a ketene and a nucleophilic imine, usually proceeds by an initial imine attack on the ketene thus forming a zwitterionic enolate which subsequently cyclizes. This reaction is an expedient route to β -lactams, the core of numerous antibiotics (e.g., penicillins) and other biologically active molecules [93]. In contrast, for Lewis-base catalyzed asymmetric reactions, nonnucleophilic imines are required (to suppress a noncatalyzed background reaction), bearing, for example, an *N*-Ts [94] or -Boc-substituent [95].

In the first step, catalyst **64c** attacks ketene **66** to form a zwitterionic enolate **71**, followed by Mannich-type reaction with imine **76** (Fig. 40). A subsequent intramolecular acylation expels the catalyst under formation of the four-membered ring. Utilizing 10 mol% of **64c**, *N*-Ts substituted β -lactams **77** were prepared from symmetrically as well as unsymmetrically substituted ketenes **66**, mainly, but not exclusively, with nonenolizable imines **76** as reaction partners [96]. Diastereoselectivities ranged from 8:1 to 15:1, yields from 76 to 97%, and enantioselectivities from 81 to 94% *ee* in the case of aliphatic ketenes **66** or 89 to 98% *ee* for ketenes bearing an aromatic substituent. Applying complexes **65** or the more bulky and less electron-rich **64b**, *ee* values below 5% were obtained.

Interestingly, the mechanistic pathway seems to change if the imine is highly electrophilic (Fig. 41): *N*-trifluoromethyl sulfonyl imines **78** react quantitatively with catalyst **64c** to form zwitterion **79** which then attacks the ketene nucleophilically similar to a regular Staudinger reaction (a similar mechanism is also likely for the formation of β -sultams [97–99]). Depending on the imine, diastereoselectivities ranged from 80:20 to 98:2. Although yields (60–89%) and enantioselectivities

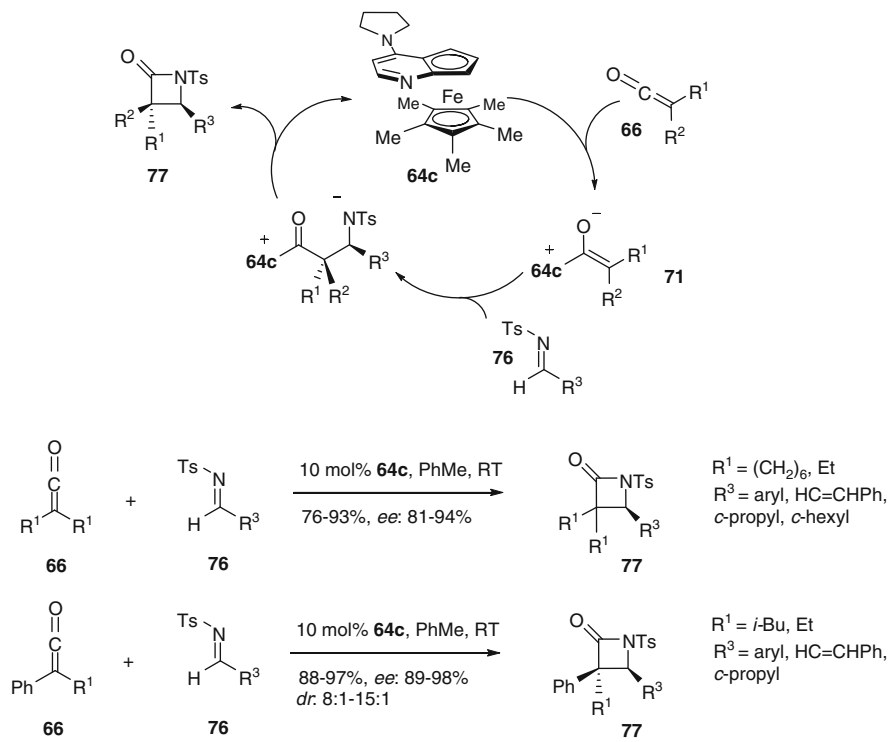


Fig. 40 Formation of β -lactams via asymmetric Staudinger-type reactions, catalyzed by **64c**

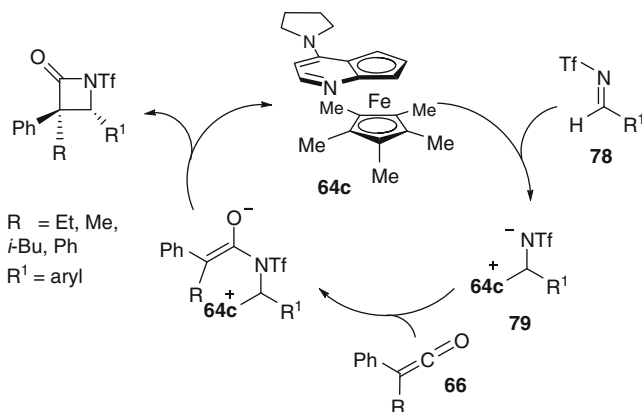


Fig. 41 Mechanistic proposal for highly electron-poor imines

(*ee* = 63–98%) were generally lower than for *N*-Ts imines **76**, both methodologies are complementary as *N*-Tf imines **78** provide, predominantly, the *trans*-diastereomers, while the *N*-Ts-counterparts **76** mainly form the *cis*-isomers.

Making use of the same reaction principle, disubstituted ketenes **66** have been reacted with aldehydes **80** to form β -lactones **81** [100], with diazo-compounds **82** to form 1,2-diazetididin-3-ones **83** [101] and with nitroso-compounds **84** to form 1,2-oxazetididin-3-ones **85** as precursors of α -hydroxy carboxylic acids (Fig. 42) [102].

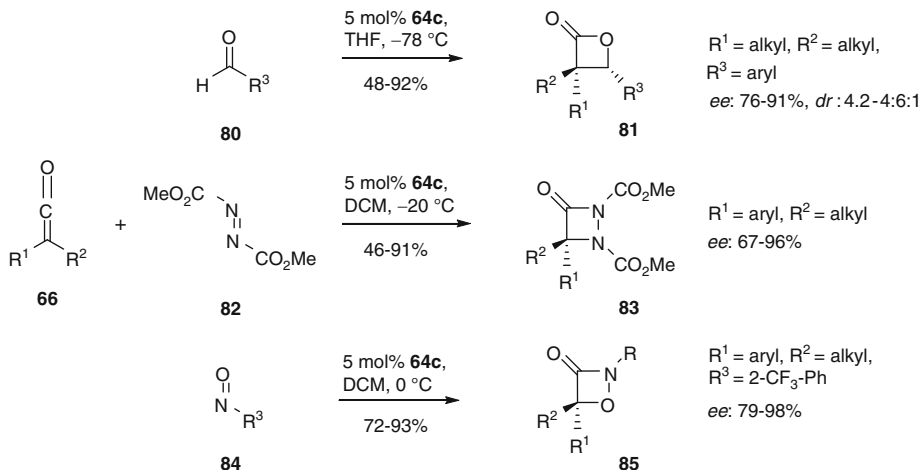


Fig. 42 Other formal [2 + 2] cycloadditions

3.2.4 Nucleophilic Catalysis: Acyl-Transfer Reactions

Enantioenriched alcohols and amines are valuable building blocks for the synthesis of bioactive compounds. While some of them are available from nature's "chiral pool", the large majority is accessible only by asymmetric synthesis or resolution of a racemic mixture. Similarly to DMAP, **64b** is readily acylated by acetic anhydride to form a positively charged planar chiral acylpyridinium species [**64b-Ac**]⁺ (Fig. 43). The latter preferentially reacts with one enantiomer of a racemic alcohol by acyl-transfer thereby regenerating the free catalyst. For this type of reaction, the C₅Ph₅-derivatives **64b/d** have been found superior.

With 1–2 mol% of **64b**, racemic mixtures of aryl-alkyl carbinols **86** [103], propargylic [104] and allylic alcohol [105] **88** and **87**, respectively, were resolved (Fig. 43). The best selectivities were attained for aryl-alkyl-carbinols **86**, where the unreacted isomer was obtained with excellent *ees* after ~55% conversion, while propargyl alcohols **88** required clearly higher conversions for high *ees* in the remaining starting material [106].

Since amines react more readily than alcohols in noncatalyzed reactions with anhydrides, the reaction is more difficult and initially required stoichiometric catalyst loadings [107], but could be performed in a catalytic sense with an O-acylated azlactone as acylating agent, which does not react with a benzylic amine at –50°C, but is capable of acylating the catalyst [108, 109]. Depending on the bulkiness of the substrate, selectivities ranged from $s = 11$ to 27 ($s = [k_{\text{enantiomer 1}}]/[k_{\text{enantiomer 2}}]$).

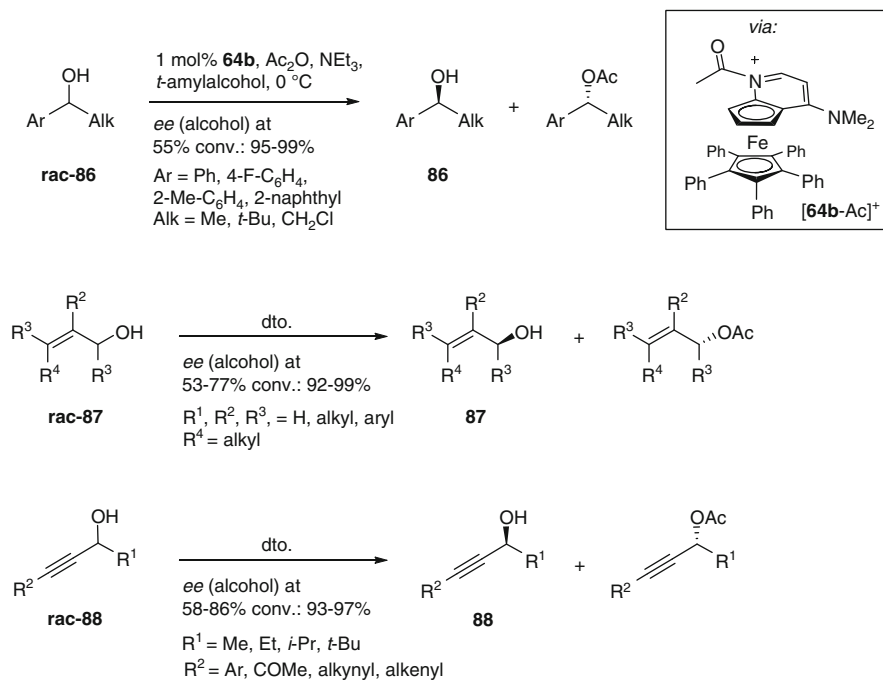
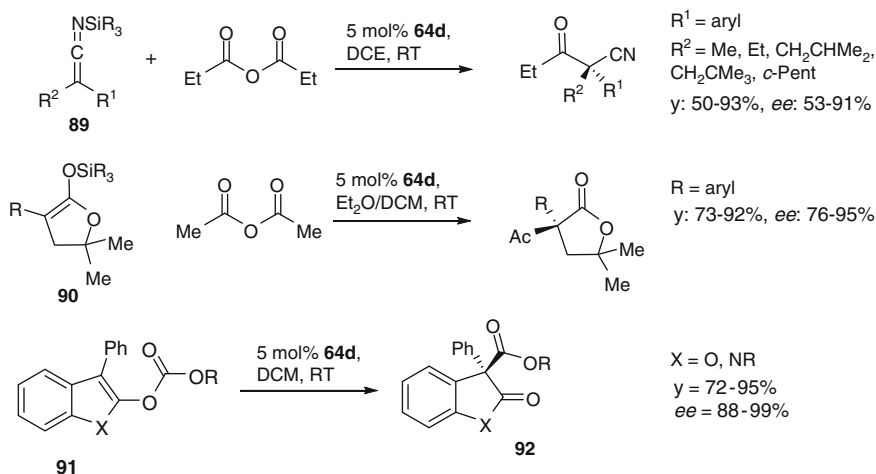


Fig. 43 Kinetic resolution via acylation of alcohols

Alternative catalytic asymmetric acylation reactions studied prochiral silyl iminoketenes **89** [110] (Fig. 44, top) and silyl ketene acetals **90** [111, 112] (Fig. 44, middle), leading to the formation of quaternary stereocenters. Furthermore, the


 Fig. 44 Further acylation reactions catalyzed by **64d**

intramolecular acyl-migration in O-acylated azlactones [113] and O-acylated benzofuranones or oxindoles **91** was reported, leading to oxindoles **92** was reported (Fig. 44, bottom) [114].

Moreover, it is possible to open racemic azlactones by acyl bond cleavage to form protected amino acids in a dynamic kinetic resolution process. As azlactones suffer a fast racemization under the reaction conditions, eventually all starting material is converted [115].

Other reactions not described here are formal [3 + 2] cycloadditions of α,β -unsaturated acyl-fluorides with allylsilanes [116], or the desymmetrization of *meso* epoxides [117]. For many of the reactions shown above, the planar chiral Fe-sandwich complexes are the first catalysts allowing for broad substrate scope in combination with high enantioselectivities and yields. Clearly, these milestones in asymmetric Lewis-base catalysis are stimulating the still ongoing design of improved catalysts.

Acknowledgment We gratefully acknowledge financial support by F. Hoffmann-La Roche (Basel).

References

1. Miller SA, Tebboth JA, Tremaine JF (1952) Dicyclopentadienyliron. *J Chem Soc* 632–635
2. Kealy TJ, Pauson PL (1951) A new type of organo-iron compound. *Nature* 168:1039–1040
3. Fischer EO, Pfab W (1952) Cyclopentadiene-metallic complex, a new type of organo-metallic compound. *Z Naturforsch B* 7:377–379
4. Ruch E, Fischer EO (1952) Binding in dicyclopentadienyliron. *Z Naturforsch B* 7:676
5. Wilkinson G, Rosenblum M, Whiting MC, Woodward RB (1952) The structure of iron bis-cyclopentadienyl. *J Am Chem Soc* 74:2125–2126
6. Woodward RB, Rosenblum M, Whiting MC (1952) A new aromatic system. *J Am Chem Soc* 74:3458–3459
7. Barusch MR, Lindstrom EG (1958) Ferrocene. US Patent 2834796
8. Lauher JW, Hoffmann R (1976) Structure and chemistry of bis(cyclopentadienyl)- ML_n complexes. *J Am Chem Soc* 98:1729–1742
9. Carter S, Murrell JN (1980) The barrier to internal rotation in metallocenes. *J Organomet Chem* 192:399–408
10. Bohn RK, Haaland A (1966) On the molecular structure of ferrocene, $Fe(C_5H_5)_2$. *J Organomet Chem* 5:470–476
11. Haaland A, Nilsson JE (1968) Determination of barriers to internal rotation by electron diffraction. Ferrocene and ruthenocene. *Acta Chem Scand* 22:2653–2670
12. Seiler P, Dunitz JD (1982) Low-temperature crystallization of orthorhombic ferrocene: structure analysis at 98 K. *Acta Crystallogr B* 38:1741–1745
13. Takusagawa F, Koetzle TF (1979) A neutron diffraction study of the crystal structure of ferrocene. *Acta Crystallogr B* 35:1074–1081
14. Rosenblum M, Abbate FW (1966) The problem of metal atom participation in electrophilic substitution reactions of the iron group metallocenes. *J Am Chem Soc* 88:4178–4184
15. Cunningham AF Jr (1994) Sequential Friedel-Crafts diacetylation of ferrocene: interannular proton transfers as a mechanistic probe. *Organometallics* 13:2480–2485
16. Watts WE (1979) Ferrocenylcarbocations and related species. *J Organomet Chem Library* 7:399–459

17. Behrens U (1979) Übergangsmetall-Fulven-Komplexe: XIV. Kristall- und Molekülstruktur von Ferrocenyldiphenylcarbenium-tetrafluoroborat, $[\text{C}_5\text{H}_5\text{FeC}_5\text{H}_4\text{C}(\text{C}_6\text{H}_5)_2]^+ \text{BF}_4^-$. Ein Fulven-Eisen-Komplex? *J Organomet Chem* 182:89–98
18. Bourke SC, MacLachlan MJ, Lough AJ, Manners I (2005) Ring-opening protonolysis of Sila [1]ferrocenophanes as a route to stabilized silylium ions. *Chem Eur J* 11:1989–2000
19. Klare HFT, Bergander K, Oestreich M (2009) Taming the silylium ion for low-temperature Diels–Alder reactions. *Angew Chem Int Ed* 48:9077–9079
20. Schlögl K (1967) Stereochemistry of metallocenes. *Top Stereochem* 1:39–89
21. Cahn RS, Ingold CK, Prelog V (1966) Specification of molecular chirality. *Angew Chem Int Ed Engl* 5:385–415
22. Whitesides TH, Shelly J (1975) Thermolysis and photolysis of (cyclopentadiene)iron tricarbonyl. Evidence for a radical mechanism involving iron(I). *J Organomet Chem* 92:215–226
23. Shackleton TA, Mackie SC, Fergusson SB, Johnston LJ, Baird MC (1990) The chemistry of $(\eta^3\text{-C}_5\text{H}_5)\text{Fe}(\text{CO})_2\text{H}$ revisited. *Organometallics* 9:2248–2253
24. Yasuda S, Yorimitsu H, Oshima K (2008) Synthesis of aryliron complexes by palladium-catalyzed transmetalation between $[\text{CpFe}(\text{CO})_2\text{I}]$ and aryl Grignard reagents and their chemistry directed toward organic synthesis. *Organometallics* 27:4025–4027
25. Jonas K, Schieferstein L (1979) Simple route to Li- or Zn-metalated η^5 -cyclopentadienyliron-olefin complexes. *Angew Chem Int Ed Engl* 18:549–550
26. Jonas K, Schieferstein L, Krüger C, Tsay YH (1979) Tetrakis(ethylene)irondilithium and Bis $(\eta^4\text{-1,5-cyclooctadiene})$ irondilithium. *Angew Chem Int Ed Engl* 18:550–551
27. Jonas K (1985) Reactive organometallic compounds obtained from metallocenes and related compounds and their synthetic applications. *Angew Chem Int Ed Engl* 24:295–311
28. Jonas K, Krüger C (1980) Alkali metal-transition metal π -complexes. *Angew Chem Int Ed Engl* 19:520–537
29. Jonas K (1990) New findings in the arene chemistry of the 3d transition metals. *Pure Appl Chem* 62:1169–1174
30. Fürstner A, Martin R, Majima K (2005) Cycloisomerization of enynes catalyzed by iron (0)–ate complexes. *J Am Chem Soc* 127:12236–12237
31. Fürstner A, Majima K, Martin R, Krause H, Kattnig E, Goddard R, Lehmann CW (2008) A cheap metal for a “Noble” task: preparative and mechanistic aspects of cycloisomerization and cycloaddition reactions catalyzed by low-valent iron complexes. *J Am Chem Soc* 130:1992–2004
32. Bonnesen PV, Puckett CL, Honeychuck RV, Hersh WH (1989) Catalysis of Diels–Alder reactions by low oxidation state transition-metal Lewis acids: fact and fiction. *J Am Chem Soc* 111:6070–6081
33. Kündig EP, Bourdin B, Bernardinelli G (1994) Asymmetric Diels–Alder reactions catalyzed by a chiral iron Lewis acid. *Angew Chem Int Ed* 33:1856–1858
34. Saha AK, Hossain MM (1993) Synthesis of a polymer-bound iron Lewis acid and its utilization in Diels–Alder reactions. *Tetrahedron Lett* 34:3833–3836
35. Olson AS, Seitz WJ, Hossain MM (1991) Transition metal catalysis of the Diels–Alder reaction. *Tetrahedron Lett* 32:5299–5302
36. Kündig EP, Dupré C, Bourdin B, Cunningham A Jr, Pons D (1994) New C_2 -chiral bidentate ligands bridging the gap between donor phosphine and acceptor carbonyl ligands. *Helv Chim Acta* 77:421–428
37. Bruin ME, Kündig EP (1998) A new chiral ligand for the Fe-Lewis acid catalysed asymmetric Diels–Alder reaction. *Chem Commun* 2635–2636
38. Kündig EP, Saudan CM, Viton F (2001) Chiral cyclopentadienyl-iron and -ruthenium Lewis acids containing the electron-poor BIPHOP-F ligand: a comparison as catalysts in an asymmetric Diels–Alder reaction. *Adv Synth Catal* 343:51–56
39. Kündig EP, Saudan CM, Bernardinelli G (1999) A stable and recoverable chiral Ru Lewis acid: synthesis, asymmetric Diels–Alder catalysis and structure of the Lewis acid macrocyclic complex. *Angew Chem Int Ed* 38:1220–1223

40. Viton F, Bernardinelli G, Kündig EP (2002) Iron and ruthenium Lewis acid catalyzed asymmetric 1,3-dipolar cycloaddition reactions between nitrones and enals. *J Am Chem Soc* 124:4968–4969
41. Bădoiu A, Brinkmann Y, Viton F, Kündig EP (2008) Asymmetric Lewis acid-catalyzed 1,3-dipolar cycloadditions. *Pure Appl Chem* 80:1013–1018
42. Bădoiu A, Bernardinelli G, Mareda J, Kündig EP, Viton F (2008) Iron- and ruthenium-Lewis acid catalyzed asymmetric 1,3-dipolar cycloaddition reactions between enals and diaryl nitrones. *Chem Asian J* 3:1298–1311
43. Bădoiu A, Bernardinelli G, Mareda J, Kündig EP, Viton F (2009) Iron- and ruthenium-Lewis acid catalyzed asymmetric 1,3-dipolar cycloaddition reactions between enals and diaryl nitrones. *Chem Asian J* 4:1021–1022
44. Artero V, Fontecave M (2008) Hydrogen evolution catalyzed by {CpFe(CO)₂}-based complexes. *C R Acad Sci II* 11:926–931
45. Itazaki M, Ueda K, Nakazawa H (2009) Iron-catalyzed dehydrogenative coupling of tertiary silanes. *Angew Chem Int Ed* 48:3313–3316
46. Sharma HK, Arias-Ugarte R, Metta-Magana AJ, Pannell KH (2009) Dehydrogenative dimerization of di-tert-butyltin dihydride photochemically and thermally catalyzed by iron and molybdenum complexes. *Angew Chem Int Ed* 48:6309–6312
47. Casey CP, Guan H (2009) Cyclopentadienone iron alcohol complexes: synthesis, reactivity, and implications for the mechanism of iron-catalyzed hydrogenation of aldehydes. *J Am Chem Soc* 131:2499–2507
48. Gómez Arrayás R, Adrio J, Carretero JC (2006) Recent applications of chiral ferrocene ligands in asymmetric catalysis. *Angew Chem Int Ed* 45:7674–7715
49. Dai LX, Hou XL (2010) Chiral ferrocenes in asymmetric catalysis. Wiley-VCH, Weinheim
50. Rigaut S, Delville MH, Losada J, Astruc D (2002) Water-soluble mono- and star-shaped hexanuclear functional organoiron catalysts for nitrate and nitrite reduction in water: syntheses and electroanalytical study. *Inorg Chim Acta* 334:225–242
51. Dupont J, Consorti CS, Spencer J (2005) The potential of palladacycles: more than just precatalysts. *Chem Rev* 105:2527–2572
52. Sokolov VI, Troitskaya LL, Reutov OA (1977) Asymmetric induction in the course of internal palladation of enantiomeric 1-dimethylaminoethylferrocene. *J Organomet Chem* 133:C28–C30
53. Kuz'mina LG, Struchkov YT, Troitskaya LL, Sokolov VI, Reutov OA (1979) Absolute configuration of the (–)-*R_p* enantiomer of cyclo-1-(1'-dimethylaminoethylferrocene)-2-(acetylacetonato)palladium. *Izv Akad Nauk SSSR Ser Khim* 7:1528–1534
54. Beletskaya IP, Cheprakov AV (2004) Palladacycles in catalysis – a critical survey. *J Organomet Chem* 689:4055–4082
55. Calter M, Hollis TK, Overman LE, Ziller J, Zipp GG (1997) First enantioselective catalyst for the rearrangement of allylic imidates to allylic amides. *J Org Chem* 62:1449–1456
56. Hollis TK, Overman LE (1997) Cyclopalladated ferrocenyl amines as enantioselective catalysts for the rearrangement of allylic imidates to allylic amides. *Tetrahedron Lett* 38:8837–8840
57. Cohen F, Overman LE (1998) Planar-chiral cyclopalladated ferrocenyl amines and imines as enantioselective catalysts for allylic imidate rearrangements. *Tetrahedron Asymmetry* 9:3213–3222
58. Donde Y, Overman LE (1999) High enantioselection in the rearrangement of allylic imidates with ferrocenyl oxazoline catalysts. *J Am Chem Soc* 121:2933–2934
59. Kang J, Yew KH, Kim TH, Choi DH (2002) Preparation of bis[palladacycles] and application to asymmetric *aza*-Claisen rearrangement of allylic imidates. *Tetrahedron Lett* 43:9509–9512
60. Moyano A, Rosol M, Moreno RM, López C, Maestro MA (2005) Oxazoline-mediated interannular cyclopalladation of ferrocene: chiral palladium(II) catalysts for the enantioselective *Aza*-Claisen rearrangement. *Angew Chem Int Ed* 44:1865–1869

61. Anderson CE, Donde Y, Douglas CJ, Overman LE (2005) Catalytic asymmetric synthesis of chiral allylic amines. Evaluation of ferrocenyloxazoline palladacycle catalysts and imidate motifs. *J Org Chem* 70:648–657
62. Kang J, Kim TH, Yew KH, Lee WK (2003) The effect of face-blocking in the enantioselective *aza*-Claisen rearrangement of allylic imidates. *Tetrahedron Asymmetry* 14:415–418
63. Overman LE, Owen CE, Pavan MM, Richards CJ (2003) Catalytic asymmetric rearrangement of allylic *N*-aryl trifluoroacetimidates. A useful method for transforming prochiral allylic alcohols to chiral allylic amines. *Org Lett* 5:1809–1812
64. Anderson CE, Overman LE (2003) Catalytic asymmetric rearrangement of allylic trichloroacetimidates. A practical method for preparing allylic amines and congeners of high enantiomeric purity. *J Am Chem Soc* 125:12412–12413
65. Nomura H, Richards CJ (2007) An investigation into the allylic imidate rearrangement of trichloroacetimidates catalyzed by cobalt oxazoline palladacycles. *Chem Eur J* 13:10216–10224
66. Prasad RS, Anderson CE, Richards CJ, Overman LE (2005) Synthesis of *tert*-leucine-derived cobalt oxazoline palladacycles. Reversal of palladation diastereoselectivity and application to the asymmetric rearrangement of *N*-aryl trifluoroacetimidates. *Organometallics* 24:77–81
67. Noviadri I, Brown KN, Fleming DS, Gulyas PT, Lay PA, Masters AF, Phillips L (1999) The decamethylferrocenium/decamethylferrocene redox couple: a superior redox standard to the ferrocenium/ferrocene redox couple for studying solvent effects on the thermodynamics of electron transfer. *J Phys Chem B* 103:6713–6722
68. Peters R, Fischer DF (2005) Preparation and diastereoselective *ortho*-metalation of chiral ferrocenyl imidazolines: remarkable influence of LDA as metalation additive. *Org Lett* 7:4137–4140
69. Peters R, Xin ZQ, Fischer DF, Schweizer WB (2006) Synthesis and Diastereoselective *Ortho*-Lithiation/Cyclopalladation of Enantiopure [2-Imidazolyl]-1',2',3',4',5'-pentamethylferrocenes and -1', 2', 3', 4', 5'-pentaphenylferrocenes. *Organometallics* 25:2917–2920
70. Weiss ME, Fischer DF, Xin ZQ, Jautze S, Schweizer WB, Peters R (2006) Practical, highly active, and enantioselective ferrocenyl-imidazoline palladacycle catalysts (FIPs) for the *Aza*-Claisen rearrangement of *N*-*para*-methoxyphenyl trifluoroacetimidates. *Angew Chem Int Ed* 45:5694–5698
71. Fischer DF, Xin ZQ, Peters R (2007) Asymmetric formation of allylic amines with *N*-substituted quaternary stereocenters by Pd^{II}-catalyzed *Aza*-Claisen rearrangements. *Angew Chem Int Ed* 46:7704–7707
72. Xin ZQ, Fischer DF, Peters R (2008) Catalytic asymmetric formation of secondary allylic amines by *Aza*-Claisen rearrangement of trifluoroacetimidates. *Synlett* 1495–1499
73. Fischer DF, Barakat A, Xin ZQ, Weiss ME, Peters R (2009) The asymmetric *Aza*-Claisen rearrangement: development of widely applicable pentaphenylferrocenyl palladacycle catalysts. *Chem Eur J* 15:8722–8741
74. Jautze S, Seiler P, Peters R (2007) Macrocyclic ferrocenyl-bisimidazoline palladacycle dimers as highly active and enantioselective catalysts for the *Aza*-Claisen rearrangement of *Z*-configured *N*-*para*-methoxyphenyl trifluoroacetimidates. *Angew Chem Int Ed* 46:1260–1264
75. Jautze S, Seiler P, Peters R (2008) Synthesis of nearly enantiopure allylic amines by *Aza*-Claisen rearrangement of *Z*-configured allylic trifluoroacetimidates catalyzed by highly active ferrocenylbispalladacycles. *Chem Eur J* 14:1430–1444
76. Jautze S, Diethelm S, Frey W, Peters R (2009) Diastereoselective bis-cyclopalladation of ferrocene-1,1'-diyl bis-imidazolines: translation of central via axial into planar chirality. *Organometallics* 28:2001–2004
77. Jautze S, Peters R (2008) Enantioselective bimetallic catalysis of Michael additions forming quaternary stereocenters. *Angew Chem Int Ed* 47:9284–9288
78. Jautze S, Peters R (2010) Catalytic asymmetric Michael additions of α -cyano acetates. *Synthesis* 365–388

79. Fürstner A, Davies PW (2007) Catalytic carbophilic activation: catalysis by platinum and gold π -acids. *Angew Chem Int Ed* 46:3410–3449
80. Chianese AR, Lee SJ, Gagné MR (2007) Electrophilic activation of alkenes by platinum(II): so much more than a slow version of palladium(II). *Angew Chem Int Ed* 46:4042–4059
81. Huang H, Peters R (2009) A highly strained planar chiral platinacycle for catalytic activation of internal olefins in the Friedel-Crafts alkylation of indoles. *Angew Chem Int Ed* 48:604–606
82. Ruble JG, Fu GC (1996) Chiral π -complexes of heterocycles with transition metals: a versatile new family of nucleophilic catalysts. *J Org Chem* 61:7230–7231
83. Wurz RP, Lee EC, Ruble JC, Fu GC (2007) Synthesis and resolution of planar-chiral derivatives of 4-(dimethylamino)pyridine. *Adv Synth Catal* 349:2345–2352
84. Nguyen HV, Butler DCD, Richards CJ (2006) A metallocene-pyrrolidinopyridine nucleophilic catalyst for asymmetric synthesis. *Org Lett* 8:769–772
85. Fu GC (2006) Application of planar-chiral heterocycles as ligands in asymmetric catalysis. *Acc Chem Res* 39:853–860
86. Wiskur SL, Fu GC (2005) Catalytic asymmetric synthesis of esters from ketenes. *J Am Chem Soc* 127:6176–6177
87. Dai X, Nikkei T, Romero JAC, Fu GC (2007) Enantioselective synthesis of protected amines by the catalytic asymmetric addition of hydrologic acid to ketenes. *Angew Chem Int Ed* 46:4367–4369
88. Hodous BL, Fu GC (2002) Enantioselective addition of amines to ketenes catalyzed by a planar-chiral derivative of PPY: possible intervention of chiral Brønsted-acid catalysis. *J Am Chem Soc* 124:10006–10007
89. Hodous BL, Ruble JC, Fu GC (1999) Enantioselective addition of alcohols to ketenes catalyzed by a planar-chiral azaferrocene: catalytic asymmetric synthesis of arylpropionic acids. *J Am Chem Soc* 121:2637–2638
90. Schäfer C, Fu GC (2005) Catalytic asymmetric couplings of ketenes with aldehydes to generate enol esters. *Angew Chem Int Ed* 44:4606–4608
91. Lee EC, McCauley KM, Fu GC (2007) Catalytic asymmetric synthesis of tertiary alkyl chlorides. *Angew Chem Int Ed* 46:977–979
92. Staudinger H (1907) Zur Kenntnis der Ketene. Diphenylketen. *Liebigs Ann Chem* 356:51–123
93. Page MI (ed) (1997) *The chemistry of β -lactams*. Chapman and Hall, London
94. Taggi AE, Hafez AM, Wack H, Young B, Ferraris D, Lectka T (2002) The development of the first catalyzed reaction of ketenes and imines: catalytic, asymmetric synthesis of β -lactams. *J Am Chem Soc* 124:6626–6635
95. Zhang YR, He L, Wu X, Shao PL, Ye S (2008) Chiral N-heterocyclic carbene catalyzed Staudinger reaction of ketenes with imines: highly enantioselective synthesis of *N*-Boc β -lactams. *Org Lett* 10:277–280
96. Hodous BL, Fu GC (2002) Enantioselective Staudinger synthesis of β -lactams catalyzed by a planar-chiral nucleophile. *J Am Chem Soc* 124:1578–1579
97. Lee EC, Hodous BL, Bergin E, Shih C, Fu GC (2005) Catalytic asymmetric Staudinger reactions to form β -lactams: an unanticipated dependence of diastereoselectivity on the choice of the nitrogen substituent. *J Am Chem Soc* 127:11586–11587
98. Zajac M, Peters R (2009) Catalytic asymmetric synthesis of β -Sultams as precursors for taurine derivatives. *Chem Eur J* 15:8204–8222
99. Zajac M, Peters R (2007) Catalytic asymmetric formation of β -Sultams. *Org Lett* 9:2007–2010
100. Wilson JE, Fu GC (2004) Asymmetric synthesis of highly substituted β -lactones by nucleophile-catalyzed [2 + 2] cycloadditions of disubstituted ketenes with aldehydes. *Angew Chem Int Ed* 43:6358–6360
101. Berlin JM, Fu GC (2008) Enantioselective nucleophilic catalysis: the synthesis of Aza- β -lactams through [2 + 2] cycloadditions of ketenes with azo compounds. *Angew Chem Int Ed* 120:7156–7158

102. Dochnahl M, Fu GC (2009) Catalytic asymmetric cycloaddition of ketenes and nitroso compounds: enantioselective synthesis of α -hydroxycarboxylic acid derivatives. *Angew Chem Int Ed* 48:2391–2393
103. Ruble JC, Tweddell J, Fu GC (1998) Kinetic resolution of arylalkylcarbinols catalyzed by a planar-chiral derivative of DMAP: a new benchmark for nonenzymatic acylation. *J Org Chem* 63:2794–2795
104. Tao B, Ruble JC, Hoic DA, Fu GC (1999) Nonenzymatic kinetic resolution of propargylic alcohols by a planar-chiral DMAP Derivative: crystallographic characterization of the acylated catalyst. *J Am Chem Soc* 121:5091–5092
105. Bellemin-Laponnaz S, Twedel J, Ruble JC, Breitling FM, Fu GC (2000) The kinetic resolution of allylic alcohols by a non-enzymatic acylation catalyst; application to natural product synthesis. *Chem Commun* 1009–1010
106. Birman VB, Li X (2008) Homobenzotetramisole: an effective catalyst for kinetic resolution of aryl-cycloalkanols. *Org Lett* 10:1115–1118
107. Ie Y, Fu GC (2000) A new benchmark for the non-enzymatic enantioselective acylation of amines: use of a planar-chiral derivative of 4-pyrrolidinopyridine as the acylating agent. *Chem Commun* 119–120
108. Arai S, Bellemin-Laponnaz S, Fu GC (2001) Kinetic resolution of amines by a nonenzymatic acylation catalyst. *Angew Chem Int Ed* 40:234–236
109. Arp FO, Fu GC (2006) Kinetic resolutions of indolines by a nonenzymatic acylation catalyst. *J Am Chem Soc* 128:14264–14265
110. Mermerian AH, Fu GC (2005) Nucleophile-catalyzed asymmetric acylations of silyl ketene imines: application to the enantioselective synthesis of verapamil. *Angew Chem Int Ed* 44:949–952
111. Mermerian AH, Fu GC (2005) Catalytic enantioselective construction of all-carbon quaternary stereocenters: synthesis and mechanistic studies of the C-acylation of silyl ketene acetals. *J Am Chem Soc* 127:5604–5607
112. Mermerian AH, Fu GC (2003) Catalytic enantioselective synthesis of quaternary stereocenters via intermolecular C-acylation of silyl ketene acetals: dual activation of the electrophile and the nucleophile. *J Am Chem Soc* 125:4050–4051
113. Ruble JC, Fu GC (1998) Enantioselective construction of quaternary stereocenters: rearrangements of O-acylated azlactones catalyzed by a planar-chiral derivative of 4-(pyrrolidino)pyridine. *J Am Chem Soc* 120:11532–11533
114. Hills ID, Fu GC (2003) Catalytic enantioselective synthesis of oxindoles and benzofuranones that bear a quaternary stereocenter. *Angew Chem Int Ed* 42:3921–3924
115. Liang J, Ruble JC, Fu GC (1998) Dynamic kinetic resolutions catalyzed by a planar-chiral derivative of DMAP: enantioselective synthesis of protected α -amino acids from racemic azlactones. *J Org Chem* 63:3154–3155
116. Bappert E, Mueller P, Fu GC (2006) Asymmetric [3 + 2] annulations catalyzed by a planar-chiral derivative of DMAP. *Chem Commun* 2604–2606
117. Tao B, Lo MMC, Fu GC (2001) Planar-chiral pyridine N-oxides, a new family of asymmetric catalysts: exploiting an η^3 -C₅Ar₅ ligand to achieve high enantioselectivity. *J Am Chem Soc* 123:353–354